Geomorphology 428 (2023) 108639

Contents lists available at ScienceDirect

Geomorphology

journal homepage: www.journals.elsevier.com/geomorphology

Modelling coarse-sediment propagation following gravel augmentation: The case of the Rhône River at Péage-de-Roussillon (France)

Daniel Vázquez-Tarrío [a,b,c,*], Alexandre Peeters [c], Mathieu Cassel [c], Hervé Piégay [c]

[a] Universidad Complutense de Madrid. Departamento de Geodinámica, Estratigrafía y Paleontología. C. de José Antonio Novais, 12, 28040 Madrid, Spain
[b] Geology Laboratory, Dpto. Producción Agraria (ETSIAAB), UPM, Madrid, Spain
[c] University of Lyon, CNRS UMR 5600 EVS, Site ENS, Lyon F-69362, France

ARTICLE INFO

Keywords:
Gravel augmentation
Sediment pulse
Gravel-bed rivers
Bedload
Sediment transport

ABSTRACT

Over the last two centuries, rivers worldwide have been affected by human interventions, including dams, river training, and gravel mining. Such actions have often involved river fragmentation and sediment starvation. In this regard, gravel augmentation is an increasingly common restoration practice for mitigating sediment starvation in gravel-bed rivers. However, uncertainties remain on how to better implement and design such operations. This is the case for the Rhône River at Péage-de-Roussillon, France, where 6885 m^3 of gravels were augmented in 2017. This work raised some concerns from river managers about the potential threat posed to a downstream reservoir from the arrival of the sediment, and explains why they were interested in the timeframe of sediment propagation, and travel distances and velocities of the augmented sediment. To answer these questions, we propose a modelling framework for simulating the long-term downstream propagation of a pulse of augmented sediment, with this framework being based on a combination of particle tracking data collected in the field and bedload transport capacity estimates. This workflow allowed us to successfully model propagation of gravels along the study reach, and provided useful information on how the sediment wave would behave over the long term. We believe that the methodology proposed in this study has much potential for exploring and investigating the kinematics of sediment wave propagation in gravel-bed rivers.

1. Introduction

Many rivers worldwide have been affected by gravel extraction over the last two centuries, as well as by the installation of dams for hydropower production, irrigation, flood control and/or water supply (Gibling, 2018). Among the many consequences of both gravel mining and dams, effects on sediment availability and continuity are some of the most conspicuous (Grant, 2012; Syvitski et al., 2022). In this regard, gravel-pits and valley closures by dams represent physical barriers that interrupt downstream transfers of sediment, leading to sediment starvation and "hungry waters" (Kondolf, 1997). Moreover, gravel mining involves a strong reduction of in-channel sediment stocks, decreasing the availability of bed material for bedload and exacerbating the effects of sediment starvation caused by sediment trapping within gravel pits and by dams (Kondolf, 1994). In addition, the flood regulation associated with dams very often involves a decrease in the frequency and magnitude of sediment transport (Schmidt and Wilcock, 2008; Dade et al., 2011; Vázquez-Tarrío et al., 2019a, 2019b). All these different disturbances to sediment fluxes may overlap and their consequences can propagate far downstream, triggering a far-reaching cascade of geomorphic and ecological adjustments that persist long after the original impact occurred. In short, both gravel mining and dams give rise to significant disruptions to sediment budgets and fluxes, with important consequences to river morphology and fluvial habitats.

The growing concerns over issues related to sediment (dis)continuity and the search for methods for the recovery of altered river habitats (e.g., the European Water Framework) have led to the implementation of numerous recent river restoration strategies aimed at mitigating the negative effects of dams and gravel mining on sediment transfers (Gaeuman, 2012). Such strategies include novel ways for regulating flow (e.g., environmental flows) (Loire et al., 2021), the installation of bypassed channels (Sumi et al., 2017), dam removal (Major et al., 2017), gravel augmentation (Bunte, 2004; Gaeuman et al., 2017; Brousse et al., 2020), and many other promising strategies for sediment management (Habersack and Piégay, 2007; Kondolf et al., 2014; Piégay et al., 2020). In this regard, gravel augmentation, i.e., the artificial replenishment of

* Corresponding author.
E-mail address: dvazqu04@ucm.es (D. Vázquez-Tarrío).

https://doi.org/10.1016/j.geomorph.2023.108639
Received 6 December 2022; Received in revised form 23 February 2023; Accepted 23 February 2023
Available online 28 February 2023

river channels with gravel and coarse sediment, is a practice increasingly common when faced with the effects of human impacts on bedload transport. Nevertheless, some questions still remain unanswered when searching for a smart design for gravel augmentation and sediment replenishment operations, as stated by Arnaud et al. (2017) and Chardon et al. (2018) in studies on the Rhine River. These questions include "what volumes of augmented gravels are the most appropriate?", "what is the most appropriate frequency (and timing) for successive gravel injections?", "where should the gravel be introduced to be efficiently entrained?", "what is the most appropriate geometry for the augmented-gravel stockpile?", and "how long will it take for the replenished gravels to reach potentially sensitive sites in terms of aggradation or flood hazards (e.g., bridges, weirs)?"

Many of these issues are not yet clearly answered, and are at least partially related to the question of how discrete deliveries of sediment propagate along a river channel or river network (Lisle et al., 1997, 2001). Indeed, aspects of sediment pulse propagation have been investigated and explored by many researchers, including topics such as the evolution of sediment pulses following landslides, debris flows (Cui et al., 2003a, 2003b), and dam removal (Cui et al., 2006a; Cui et al., 2006b; Gilet et al., 2021), but they have only rarely been considered in the context of gravel augmentation (Sklar et al., 2009). Over recent decades, several numerical models have been developed for simulating and predicting the propagation of coarse-sediment pulses along river channels, including the Dam Removal Express Assessment Model (DREAM) (Cui et al., 2006a; Cui et al., 2006b), the Unified Gravel-Sand Model (TUGS) (Cui, 2007), the Morphodynamics and Sediment Tracers in 1D model (MAST 1D) (Lauer et al., 2016), the Lagrangian framework proposed by Czuba (2018) and Ahammad et al. (2021), or the recent numerical model proposed by Viparelli et al. (2022). Many of these morphodynamic models focus on the aggradation/degradational response of the riverbed and provide an estimate of bed level changes through time. However, they are not designed to track the movement of individual particles, which in the case of gravel augmentation is of particular interest given the need for information on the timeframe of sediment evacuation before arriving at potentially sensitive areas. This concern applies, for instance, to the DREAM (Cui et al., 2006a; Cui et al., 2006b), TUGS (Cui, 2007) or MAST 1D (Lauer et al., 2016) models. Some recent developments (e.g., Czuba, 2018; Ahammad et al., 2021; Viparelli et al., 2022) are promising in their ability to track the downstream propagation of sediment but, in our opinion, still remain focused on estimating bed response. There is also a need to better constrain certain model parameters using more experimental or field data.

In this regard, most of these models were derived from purely mathematical/theoretical lines of reasoning or were developed based on observations collected from flume experiments. Although it is true that many of them have been validated with field data (e.g., the Navarro River in Cui et al., 2006a, 2006b; the Ain River in Lauer et al., 2016; the Buëch River in Viparelli et al., 2022), in almost none of these models is information derived directly from field observations collected in rivers used in the calibration or in the definition of model parameters, which represents a major limitation. To the best of our knowledge, this fact is likely related to the lack of robust and strong functional relations linking water discharge to the distances or velocities of sediment propagation observed in the field (Hassan and Bradley, 2017; Klösch and Habersack, 2018; Papangelakis et al., 2022), which is indeed an elusive (although longstanding) topic in river research. In this regard, particle tracking has probably been the most popular strategy for the field study of fluvial gravel displacement (and dispersion) along river channels (Hassan and Roy, 2016), and much research effort has been invested in tracking particle displacements in gravel-bed rivers using tagged stones. Such tracer research has helped to disentangle the nature of the multiple controls behind gravel transport (Hassan and Bradley, 2017; Vázquez-Tarrío et al., 2019a, 2019b; McQueen et al., 2021), which include the magnitude and duration of discharge (Phillips and Jerolmack, 2014; Houbrechts et al., 2015; Papangelakis et al., 2022), channel morphology (Pyrce and Ashmore, 2003; McQueen et al., 2021; Peeters et al., 2021), macro-bedforms (Vázquez-Tarrío et al., 2019b), grain-size (Church and Hassan, 1992), active-layer fluctuations (Haschenburger, 1999; Vázquez-Tarrío et al., 2021), and the length scale of the channel (Beechie, 2001; Vázquez-Tarrío and Batalla, 2019). All this previous work has undoubtedly contributed to providing us with a clearer idea on how bedload behaves and how the controls on gravel displacements observed in the field largely depend on the scale of the study (Vázquez-Tarrío and Batalla, 2019). At the river-reach scale, clast displacements are mainly controlled by hydraulics, i.e., discharge and flow duration, whereas when different rivers and reaches are compared, factors such as the planform morphology or the length of the channel may eventually explain equal or greater variance in gravel displacements than the variability explained only by the water flow (Beechie, 2001; Vázquez-Tarrío and Batalla, 2019). So, the difference between cause and effect depends on the scale of the study (Schumm and Lichty, 1965), precluding the establishment of generalizable and/or robust regression models allowing the estimation of travel displacements on the basis of hydraulic parameters alone.

In the present paper, we address the problem of the dispersion/translation of a pulse of augmented gravel in a river and propose a relatively simple 1D workflow for predicting coarse sediment propagation following gravel augmentation. The proposed workflow combines the computation of bedload volumes using sediment transport equations with the estimation of particle displacements based on field data obtained from particle tracking. In this regard, the two main strengths of our modelling approach are its capacity for 'tracking' downstream sediment displacements, and the use of field data (from particle tracking) to constrain the model parameters. To demonstrate this combined numerical/field-based approach, we applied it to the Rhône River at Péage-de-Roussillon (France), a heavily managed river reach where restoration works accomplished in 2017 involved the injection of 6885 m^3 of gravel. We believe that the proposed workflow provides a relatively simple but well-suited strategy for modelling sediment pulse propagation following gravel replenishment, and may be of interest to those researchers interested in improving the design of gravel augmentation works in rivers.

2. Study site and the context for the present research

The Rhône River is one of Europe's major rivers, representing, on average, one sixth of the annual runoff into the Mediterranean Sea. The Rhône originates at the Rhône Glacier in the Swiss Alps, and after discharging into Lake Geneva (approximately 200 km downstream from its source), it crosses into France and flows 512 km before reaching the Camargue delta and the Mediterranean Sea. The Rhône River drains a catchment area of ~98,000 km^2 (90,500 km^2 within France), and its mean annual discharge varies from about 200 m^3/s at Lake Geneva to 1700 m^3/s near the river's mouth. In the present research, we focus on a 30-km reach of the French Rhône located close to the town of Péage-de-Roussillon (Fig. 1). The average slope and width of this reach are 0.001 and 230 m, respectively. The average D_{50} and D_{84} of the surface grain size distribution are 48 and 76 mm, respectively, and the measured armor ratios vary between 1.3 and 6.7. The mean annual and 2-yr peak discharges are 1010 m^3/s and 3300 m^3/s, respectively (Vázquez-Tarrío et al., 2022).

The Rhône River, particularly the French section, has a long history of intense river management dating back to the end of the nineteenth century, and which has involved river navigation, embankments, gravel extractions, and hydropower production (Parrot, 2015; Vázquez-Tarrío et al., 2022). Over the last decade, several restoration works were carried out within the framework of the Rhône management Plan (2010–2015) and the Rhône-Mediterranean SDAGE (2017–2021), with the objective of recovering part of the sediment fluxes and improving the ecological quality of the river.

The aforementioned management history also applies to the reach

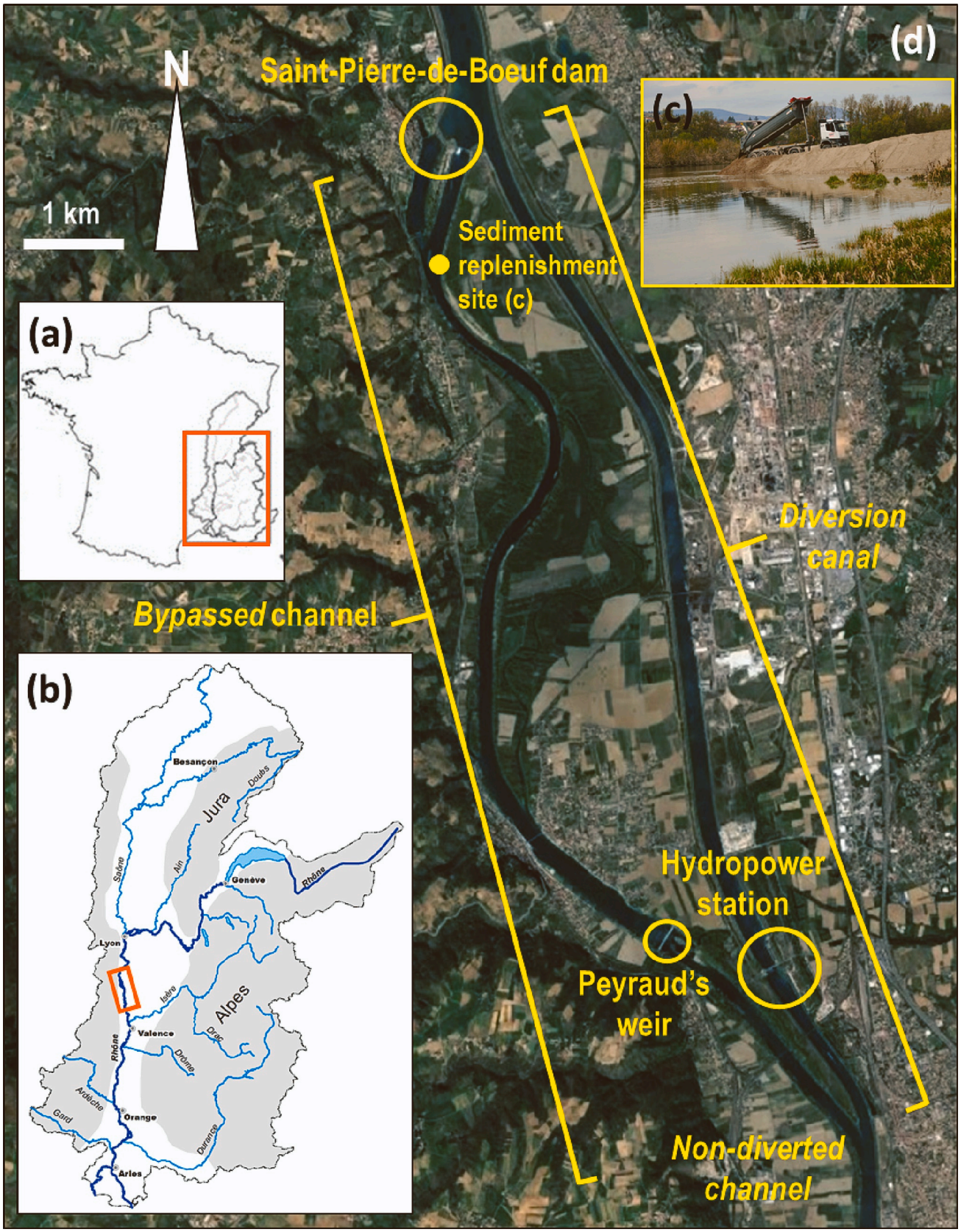

Fig. 1. (a) Location of the Rhône's drainage basin within France. (b) Location of the study site within the Rhône's drainage basin. (c) Field photograph of the augmented sediment stock pile (courtesy of Bernard Pont). (d) Aerial image of the study site (source: Google Earth), outlining the main features of the hydropower management scheme.

studied in this work (Fig. 1C); it was narrowed and embanked at the beginning of the twentieth century with the aim of improving river navigation. Between 1970 and 1972, a diversion run-of-river dam was constructed in the downstream section of the study reach (Arras dam), and another one (Saint-Pierre-de-Bœuf dam) was built in the upstream section between 1972 and 1979. The latter diverts a substantial amount of the discharge into a diversion canal, where the water is used for hydropower production before being returned to the main Rhône channel approximately 12 km downstream. As a result, the magnitude and frequency of moderate to large flows are substantially reduced in the bypassed channel, with an average discharge of approximately 120 m^3/s compared with the 1015 m^3/s in the non-diverted channel. The Saint-Pierre-de-Bœuf dam did not only impact the flow discharge, but also the sediment supply into the bypassed reach. Although sluice gates are opened during large floods and sediment can partially travel into the bypassed reach, the reality is that flow diversion significantly reduced the frequency of bedload transport in the study reach. Consequently, the present-day annual bedload rates are estimated to be 2–3 times lower than they were in the pre-management conditions (Vázquez-Tarrío et al., 2019a, 2019b). Furthermore, a weir (Peyraud weir) was built in 1978 in the bypassed channel, approximately 10 km downstream of the Saint-Pierre-de-Bœuf dam, to maintain the water table level.

Within this general management context, 6885 m^3 of gravel were extracted from the river margins and introduced into the main channel in 2017 with the aim of restoring bedload transport within this reach, and thus improving river habitats. This operation was initially intended to increase existing gravel availability in the reach and mobilize the armoured bed. Nevertheless, this gravel-augmentation operation raised two important questions for the company in charge of managing the dams, the Compagnie Nationale du Rhône (CNR). First, because the CNR is legally responsible for ensuring the safety of the reservoirs, they were concerned about the effects on the flood risk in adjacent areas. Indeed, large volumes of sediment could quickly reach the reservoir of the downstream dam, raising the riverbed level and decreasing the channel conveyance capacity, which could locally lead to an increase in the risk of flooding. The second concern was the duration of the beneficial effects of the replenishment actions on river habitats and whether or not a single injection would have long-term sustained effects on the bypassed channel.

3. Material and methods

3.1. Rationale

As stated above, the main aim of the present work was to compute the rate at which a pulse of augmented gravels introduced in 2017 will propagate along the Rhône River channel over the long term. To address this issue, we considered that the propagation of the replenished sediment could be mainly explained by a combination of two mechanisms: first, the entrainment of the augmented gravels into the bedload; and second, the downstream displacement of the recruited sediment by the water flow. Consequently, we considered that the problem of estimating the time required for a certain volume of augmented gravels to travel along the Rhône channel could be reduced or simplified to finding the answers to these two questions: (1) what is the rate at which the gravels are entrained by the water flow? and (2) what are the distributions of the distances travelled downstream by the recruited sediment?

The first question relates to an Eulerian (at-a-site) approach to bedload transport, and is a question that is classically addressed by means of sediment-transport equations; indeed, there is a longstanding tradition searching for a functional link between bulk bedload volumes and section-averaged hydraulic parameters in river hydraulics research (Recking, 2013). As a result, there are plenty of available equations that provide more or less reliable estimates of bedload rates (Vázquez-Tarrío and Menéndez-Duarte, 2015; Hinton et al., 2018). The second question relates to the Lagrangian approach to bedload transport, and is a much more complex problem because of the lack of comparable formulae linking travel distances to discharge (Papangelakis et al., 2022). This is caused in large part to the complex nature of gravel propagation, involving a combination of translation, diffusion, and dispersion (Lisle et al., 2001). Nevertheless, previous particle tracking studies may provide some keys to addressing this question.

Based on the above-described approaches and information, we proposed a one-dimensional modelling workflow for simulating the propagation of replenished sediment in the study reach. This modelling involves four different steps (Fig. 2): (1) establishing an adequate modelling grid; (2) defining bedload transport capacities at each node of the modelling grid; (3) estimating the distribution of downstream travel distances for the injected gravels at each node; and (4) combining points (2) and (3) to predict propagation of the augmented sediment along the modelling grid from the upstream to downstream nodes.

3.2. Creation of the model grid

The first step for the model implementation was creation of the model grid. Our proposed model framework is one-dimensional, with the grid consisting of a set of nodes, each corresponding to a channel cross section. The most upstream node of the model grid corresponds to the location or channel section where gravel augmentation occurred, and the most downstream node corresponds to the downstream Arras dam. Our modelling approach is compatible with regular or irregular model grids. For simplicity, and to save computing time, we used a regular grid. Each node of the model grid is associated with the section-averaged values of all the parameters (e.g., width, slope, and grain size) needed for bedload computation. Bathymetric data collected between 1999 and 2010 were available (in numerical form) through the "BDT Rhone" (Rhône Topographic Data Base), compiled as part of the "Plan Rhône", and managed and distributed by IGN (Institut national de l'information géographique et forestière). As the available bathymetric data contained topographic data for a cross section every 500 m, the initially created grid involved a 500-m spacing between nodes, one node for each available cross section.

However, the successful application of the workflow that we propose here required careful consideration of what the best spacing between nodes should be. The spacing between nodes must have a proportional relationship with the mean travel length of the sediment because a larger spacing is more likely to involve sediment deposition between the nodes; i.e., if the spacing between the nodes is larger than the distance travelled by the sediment, we could expect that large volumes of sediment would be recorded as being trapped within the nodes immediately downstream of the departing point. Therefore, to avoid potential artifacts in the modelling of sediment storage between nodes, the grid spacing should be shorter than the average travel lengths of the

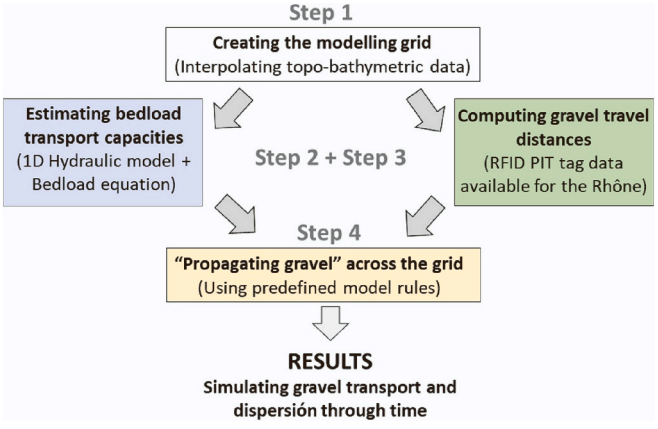

Fig. 2. Workflow followed in the present research for modelling the long-term propagation of augmented gravels in the study site.

augmented sediment. In this regard, the original 500-m spacing between nodes seemed rather large considering the order of magnitude of travel distances reported by the tracer surveys available for the study site (approximately 50–100 m/yr, see information below). Consequently, we decided to increase the resolution of the model grid by interpolating the bathymetric information and creating one node every 50 m. Nevertheless, we also tested the model's sensitivity to different grid spacings (10, 25, 100, 250, and 500 m).

3.3. Defining bedload transport capacities at each node

The second step of the model implementation consisted of associating a value for the average annual bedload transport capacity with each node of the model grid. For this, we benefited from the results of a previous study (Vázquez-Tarrío et al., 2019a) in which bedload transport rates were estimated for the entire French Rhône River (512 km). In this previous work, a 1D-hydrodynamic model based on the numerical software MAGE was used to predict the water line (slope, velocity) for different values of discharge along the river. The MAGE software simulates open channel flows in transient regimes by solving the 1D Barré-de-Saint-Venant (shallow water) equations using a four-point finite difference scheme (Preissmann scheme). The model was calibrated and validated by Dugué et al. (2015), Launay et al. (2017), and Le Coz et al. (2021), using water slope and water level data for the Rhône River for a wide range of discharges. The outcomes of this hydraulic model were available for the present research. Readers are referred to the previous works for more information on the hydraulic model.

The outputs of the 1D-hydrodynamic model included section-averaged water velocity and slope at each cross section of the Rhône River (cross section spacing of 100 m). They were used to estimate shear stresses and compute bedload transport rates for the different bins of discharge of the flow duration curve of the study reach. The sediment transport equation of Recking (2013) and Recking et al. (2016) was used for this purpose. This equation was chosen because it was previously reported to provide reliable bedload estimations in gravel-bed rivers (Hinton et al., 2018; Vázquez-Tarrío and Menéndez-Duarte, 2021) such as the Rhône River. Furthermore, Vázquez-Tarrío et al. (2019a, 2019b) tested four different equations in the Rhône (Meyer Peter and Müller, 1948; Wilcock and Crowe, 2003; Camenen and Larson, 2005; Recking et al., 2016), and found that the equation of Recking et al. (2016) provided bedload volumes consistent with the bed sediment budgets reported by Dépret et al. (2019). This equation computes the bulk volume bedload rate q_s as:

$$q_s = 14 \bullet \sqrt{g \bullet 1.65 \bullet D_{84}^3} \bullet \frac{\tau^{*2.5}}{1 + \left(\frac{\tau^*_m}{\tau^*}\right)^4} \bullet w \quad (1)$$

where g is the acceleration due to gravity, w is the active channel width, D_{84} is the 84th percentile of the grain size distribution, τ^* is the Shields shear stress, and τ^*_m is the reference Shields stress separating partial from full mobility conditions. Shields stress is estimated from:

$$\tau^* = \frac{S \bullet R}{1.65 \bullet D_{84}} \quad (2)$$

where S is the slope and R the hydraulic radius. The reference Shields stress τ^*_m is estimated from the expression:

$$\tau^*_m = (5 \bullet S + 0.06) \bullet \left(\frac{D_{84}}{D_{50}}\right)^{4.4 \bullet \sqrt{S} - 1.5} \quad (3)$$

where D_{50} is the median size of the grain size distribution.

In the present work, we were interested in estimating the capacity of the channel to convey the augmented gravels. Therefore, we used the grain size distribution of the replenished sediment in Eqs.(1) to (3). To do this, the bulk mass grain size of the replenished sediment was measured at its source (Fig. 3A). We also used Eqs. (1)–(3) to estimate bedload transport capacities for the grain size metrics of the streambed sediment to obtain an idea of the mobility of the riverbed sediment. In this regard, 10 bulk mass samples were collected in this reach as part of a field campaign carried out by the Rhône Sediment Observatory (OSR)

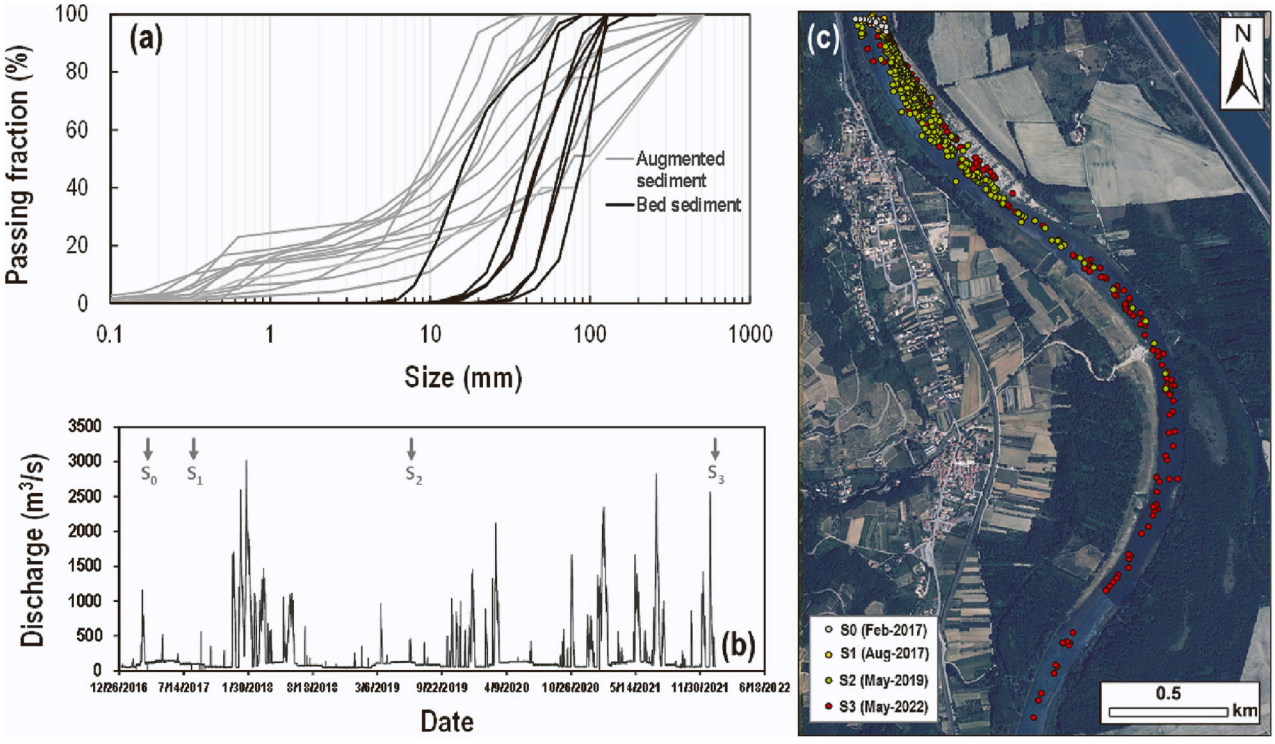

Fig. 3. (a) Grain size distribution information available for the study reach. (b) Water discharges in the study reach during the time spanned by the present research. (c) Particle tracking data collected in the study reach for the present research.

between 2011 and 2013 in collaboration with the CNR. Grain size sampling was conducted from a boat using a triangular dredge with frame dimensions of 50 × 50 × 50 cm (Vázquez-Tarrío et al., 2022). As in Vázquez-Tarrío et al. (2019a, 2019b), linear interpolation was performed between samples to provide an estimate of grain size for all transects modelled with the 1D hydraulic model.

For all this work, we benefit from the hydrometric data and the flow duration curve for the study reach provided by the Regional Environment Planning and Housing Agency (DREAL) and the CNR (the company that manages the upstream and downstream dams). Then, the 1D hydraulic model was run for different bins of discharge of the flow duration curve. The outputs (energy slope, hydraulic radius) of the 1D hydraulic model were used to compute the section-averaged bed shear stresses at each node of the model grid. Later, these estimates were introduced, together with available grain-size information, into Eqs. (1) to (3) to compute the bedload transport rates for different discharges of the flow duration curve, which in turn were weighted by their frequency of recurrence to estimate the average annual bedload volumes at each node of the model grid. This procedure follows that used in Vázquez-Tarrío et al. (2019a, 2019b) to estimate bedload transport capacities in the Rhône River, and readers are again referred to this previous research for more detailed information on the way bedload volumes were estimated. Mean annual bedload volumes of 6300 m^3 were computed for the bed sediment in the study reach, while bedload transport capacities of 10,250 m^3 were estimated for the augmented gravel.

3.4. Defining particle travel distances at each node

The next step was to define values for the potential distances of travel of the augmented gravel for each node of the model grid. In this regard, the plume of augmented gravel will travel downstream by a combination of translation and dispersion (Lisle et al., 1997, 2001; Gaeuman et al., 2017), and therefore, instead of defining a single value for the travel distance at each node, we needed to specify a distribution of frequencies for the travel distances.

Previous research reported that travel lengths tend to follow either an exponential or a gamma distribution (Hassan et al., 1991; Lamarre and Roy, 2008; Bradley & Tucker, 2012; Liébault et al., 2012; Hassan et al., 2013; Phillips and Jerolmack, 2014; Olinde and Johnson, 2015; Papangelakis and Hassan, 2016). In principle, an exponential distribution best describes situations where a large proportion of particles remain immobile or move only short distances, whereas a gamma distribution is best suited to cases where many particles travel far from their seeding locations (Hassan et al., 1991; Pyrce and Ashmore, 2003; Papangelakis et al., 2022). The exponential probability distribution is a single parameter distribution, requiring only the definition of the rate parameter λ:

$$P(L) = \lambda \bullet e^{-\lambda \bullet L} \tag{4}$$

where $P(L)$ is the probability of a given travel length L. The rate parameter λ is the inverse of the distribution mean, i.e., the mean travel length. Once the mean travel distance of the augmented gravels is known, it is possible to define the entire travel length distribution if it is exponentially distributed. On the other hand, the gamma distribution is a two-parameter distribution, requiring the definition of the shape α and scale β:

$$P(L) = \frac{\beta}{\Gamma(\alpha)} \bullet L^{\alpha-1} \bullet e^{-\beta \bullet L} \tag{5}$$

The α and β parameters are related to the distribution mean (i.e., the mean travel length) and variance according to:

$$\frac{\alpha}{\beta} = \overline{L} \tag{6}$$

and

$$\frac{\alpha}{\beta^2} = \sigma^2 \tag{7}$$

where $\overline{L}$ is the mean travel length and σ^2 is the variance of tracer displacements. Therefore, in the case of the gamma distribution, knowledge of the mean travel distance is insufficient to infer the entire travel length distribution, and it is also necessary to know the variance of the travel distances.

In both the exponential and gamma distributions, the mean travel distance of the augmented gravels is a key parameter for fitting the distribution and recovering the travel length distribution at each node. Unfortunately, no previous research has found a relatively simple and universal relation linking the mean travel distances of fluvial sediment to peak discharge or basic hydraulic parameters. In fact, previous research showed how mean travel distances depend on both peak discharge and the duration of flow (Phillips et al., 2018; Gervasi et al., 2021), but this relation shows a large variability and tends to be site specific (Haschenburger, 2013; Papangelakis and Hassan, 2016; Papangelakis et al., 2022). Nevertheless, Haschenburger (2013), Papangelakis and Hassan (2016) and Papangelakis et al. (2022) observed that mean travel distances are locally well correlated with the excess stream power or energy according to linear or power relationships of the kind:

$$\overline{L} = a \bullet \Omega^b \tag{8}$$

where a and b are the empirical intercept and coefficient, respectively, and Ω represents the cumulative excess energy or time-integrated stream power computed as:

$$\Omega = \rho \bullet g \bullet S \bullet \int_{t_o}^{t_f} (Q_t - Q_c)dt \tag{9}$$

where ρ is the density of water, S is the bed slope, Q_t is the water discharge at an instant t, Q_c is the critical discharge, and t_0 and t_f are the start and end of the mobilizing event. The regression model represented by Eq. (8) provides good estimations of mean travel lengths when applied to individual sites once the values of a and b have been locally fitted. The values of b reported in previous studies range from 0.6 to 1.25 (Haschenburger, 2013; Papangelakis and Hassan, 2016; Bradley, 2017; Papangelakis et al., 2022).

To calibrate the model described by Eq. (8) for the Rhône, we used information on gravel displacements obtained with PIT (Passive Induced Transducers) tagged stones deployed by the river consultants Geopeka (2019) and later surveyed by them and Peeters et al. (2022). Thus, on 14 March 2017, after the stockpile of augmentation gravel had been introduced, 991 tracer stones tagged with RFID (Radio-frequency identification) PIT labels (PIT tags of 12, 23, and 32 mm in length) were seeded into the sediment stockpile. A specific water-drilling technique was applied (Geopeka, 2019) that allowed small particles to be drilled. The tracer stones covered five particle size classes: 8–16 mm, 16–32 mm, 32–45 mm, 45–64 mm and 64–90 mm. The tracer stones were seeded in 20 clusters of about 60 tracers, and were distributed in the channel and on the top of the stockpile of augmented sediment. Three surveys combining pedestrian and boat prospection were carried out on August 2017 (S1), May 2019 (S2), and May 2022 (S3). For these surveys, we used two different antennas (Arnaud et al., 2015), a large rectangular antenna (2 m by 0.5 m) that was dragged from a boat (in deep areas) or by two operators (on emerged banks and in shallow areas), and a small circular antenna (0.5 m in diameter) that was swept by an operator in shallow areas or places with a lot of vegetation. The distances travelled by tracer stones were measured by projecting tracer positions onto the channel centerline, and the displacements were measured as streamwise distance along the channel relative to the original seeding point.

Peak flows between the tracer seeding (S0, February 2017) and the first survey (S1) were relatively low, reaching a maximum peak

discharge of 526 m^3/s and a cumulative flow duration (above critical) of less than three days (Fig. 3B). As expected, the measured tracer displacements were also low during this period (mean and maximum travel distances of 7 and 32 m, respectively). Tracer recovery was also low (8 % of recovered tracers), probably because of weak tracer displacements and signal collisions between very close PIT tags. The period between S1 and S2 was characterized by three successive flood peaks reaching 1712, 2600, and 3021 m^3/s. Tracer recovery was higher (39 %) than for the previous period, and tracer displacements (mean and maximum tracer displacements of 415 and 2080 m, respectively) were also higher for this study period (Fig. 3C). Finally, the period between S2 and S3 was marked by four successive peaks of flow reaching 2117, 2344, 2744, and 2466 m^3/s (Fig. 3B). Yet again, we measured significant tracer displacements during this period (Fig. 3C), with mean and maximum displacements (from the initial seeding point) of 928 and 3652 m, respectively.

Table 1 summarizes the recovery statistics by size fraction of the different surveys. To maximize information on lost tracers, we employed the PITtrack2 Matlab code developed by MacVicar and Papangelakis (2022). This tool maximizes the information that can be obtained from a series of particle tracking surveys when the tagged stones are intermittently lost and re-found. Following the recommendations of MacVicar and Papangelakis (2022), we included two classes of lost tracers into the analysis of our data: (1) 'intersect' tracers: stones found in two successive surveys; and (2) 'inferred' tracers: tracer stones missing in a given survey but re-found close to their previously known position in a later prospection, allowing us to infer that they were immobile.

In Table 2 we summarize the travel-length metrics for the three surveys. The information on travel lengths obtained from the tracer surveys was used to calibrate Eq. (8) for the study reach, which in turn required defining the value of the critical discharge. The relatively low tracer displacements measured during the first survey suggest that the peak discharges reached during the first study period were close to the critical discharge. We then compared the values of discharge before and after the first tracer displacements were observed to obtain an idea of the maximum peak discharge without tracer displacement. We used data from the gauge at the St. Pierre de Boeuf dam provided by CNR, which included hourly discharge for the study reach from January 2015 to January 2022. The inferred discharge (525 m^3/s) was used as a reference value or first approximation of the critical discharge. Additionally, we estimated the intersect of the regression line linking the mean travel distance to the peak discharge on the x-axis. We obtained a value of 468 m^3/s, which is close to our previous inferred value for a critical discharge of approximately 500 m^3/s. Finally, we also estimated the critical discharge at the injection point using Recking's (2013) approximation of the critical Shields stress (τ_c^*) for heterogenous gravel-bed rivers:

$$\tau_c^* = 1.32 \bullet S + 0.037 \quad (10)$$

The computed value is 530 m^3/s, which is not very far from the critical discharge inferred from tracer displacements (~500 m^3/s). This suggests that Eq. (10) could be a good approximation of the threshold discharge in the study reach.

Based on the observed tracer displacements, the estimated critical discharge, and the available hydrological data, we fitted the regression model described by Eq. (8) (Fig. 4) and observed a statistically significant strong correlation ($R^2 = 0.99$, p-value <0.05) between the mean tracer displacements for the different surveys and the cumulative flow energy. The observed value for the model exponent was 0.52, which is close to the 0.49 exponent documented by Schneider et al. (2014), but slightly lower than the values typically reported in previous literature, which range between 0.65 (Bradley, 2017) and 1.24 (Papangelakis and Hassan, 2016). Nevertheless, the observed data are also congruent with a purely linear model ($R^2 = 0.99$, p-value <0.05) (Fig. 4), as observed in other studies (Haschenburger, 2013; Papangelakis and Hassan, 2016; Papangelakis et al., 2022).

Concerning the influence of grain size on travel distance, in principle, our data do not show major differences in the magnitude of tracer displacements according to tracer size. However, this result must be taken with caution given the low percentage of recovery of the finest size classes, as it does not exclude the possibility of these classes having been displaced over distances greater than those prospected. Moreover, the median size (~72 mm) of riverbed sediment was coarser than the tagged stones at the site where tracers were seeded. In this regard, previous tracer studies reported how the size of sediment particles relative to the overall distribution of sizes within the channel bed influences particle travel distance (Church and Hassan, 1992). The analysis accomplished by Church and Hassan (1992) clearly demonstrated that grain size has an influence on the downstream transport distances of particles coarser than the median grain size of the riverbed, whereas travel distances for particles finer than the median size of the bed sediment are less influenced by clast size.

In Fig. 5, the observed tracer travel distances scaled by the mean distance of travel of the median size class of surface sediment (L^*) are plotted against the ratio of the tracer size to the median size of the surface grain size distribution (D^*). We compared tracer data for the study reach with the general relationships between tracer travel distances and tracer size proposed by Church and Hassan (1992), Milan (2013), and Vázquez-Tarrío et al. (2019a, 2019b), which were based on compiled data from previous tracer studies. In general, the Rhône River data show high scatter, and tend to show an opposite trend to that observed in previous works; indeed, the travel distances increased

Table 1
Recovery metrics for the different tracer surveys. N_0: Number of initially seeded tracers. N: Number of retrieved tracers. RR: Tracer recovery ratio.

Size class (mm)	N_0	Survey 1		Survey 2		Survey 3	
		N	RR (%)	N	RR (%)	N	RR (%)
8–16	236	9	3.8	55	23.3	32	13.6
16–32	260	14	5.4	88	33.9	59	22.7
32–45	196	22	11.2	87	44.4	78	39.8
45–64	201	22	10.9	104	51.7	94	46.8
64–90	96	15	15.6	51	53.1	47	49.0

Table 2
Displacement metrics for the different tracer surveys. L_{mean}: Mean travel distance from initially seeding point. L_{max}: Maximum travel distance. SD: Standard deviation of travel distances. N_{rec}: Number of recovered tracers. RR: Tracer recovery ratio.

Survey	Date	L_{mean} (m)	L_{max} (m)	SD (m)	N_{rec}	RR (%)
1	August-2017	7	32	4	82	8
2	May-2019	415	2080	336	385	39
3	May-2022	928	3652	936	310	31

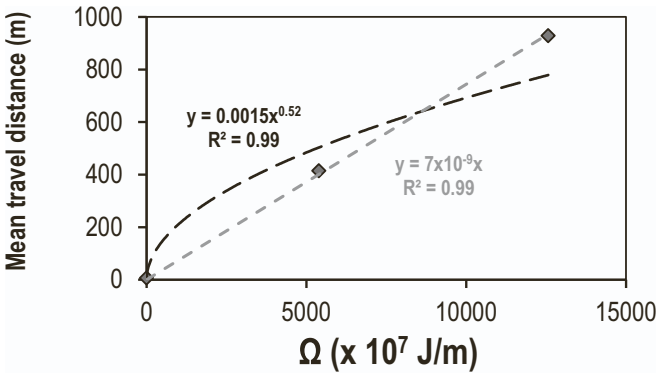

Fig. 4. Best power and linear fit between the mean travel distance and cumulated flow energy reported for the available tracer data in the study reach.

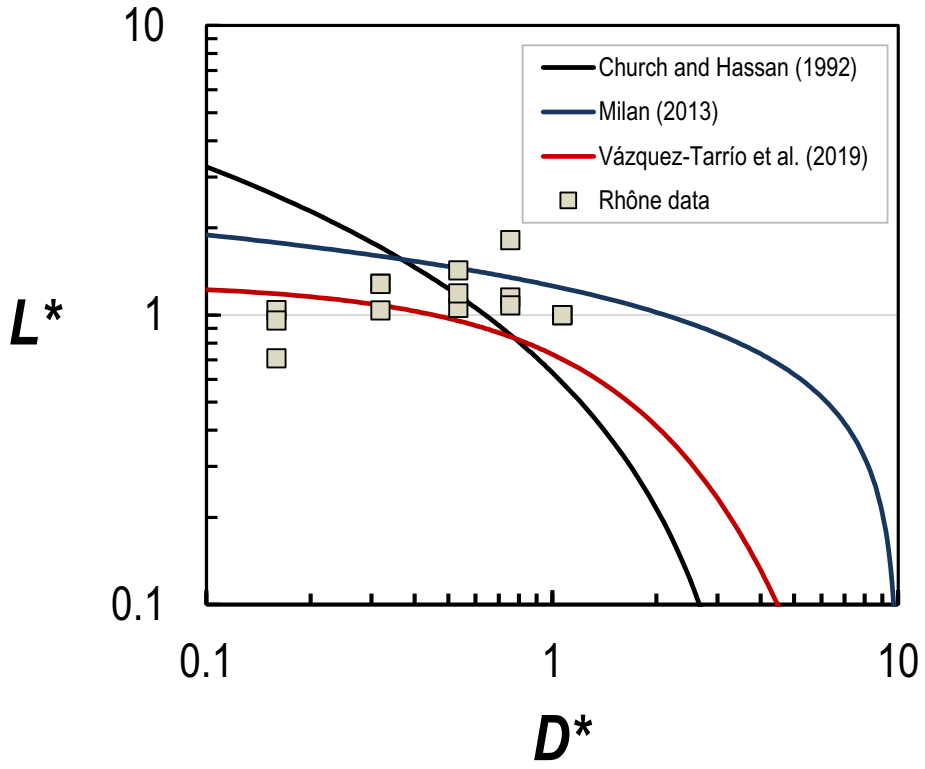

Fig. 5. Mean travel length of tracers of different size classes plotted against grain size. Travel lengths were normalized by the mean travel length of tracers corresponding to the size class of the median size of bed sediment (L^*). Grain sizes were normalized by the median size of bed sediment (D^*). Available data for the study reach were compared with the trends observed by different authors.

slightly with grain size, which seems counterintuitive. This observation is probably related to poor retrieval of tracers in the 8–16 mm and 16–32 mm size classes. Clasts in these size classes were equipped with 12- and 23-mm PIT tags that normally have lower detection ranges than the 32-mm PIT tags used for the larger size classes. Therefore, the results are probably biased by this fact and the mean travel distances for these size classes were probably larger. Accounting for this, the Rhône data could be considered as being coherent with regression lines between the travel distance and particle sizes observed by Milan (2013) and Vázquez-Tarrío et al. (2019a, 2019b). On the basis of this observation, we decided to correct the mean travel distances estimated at each node (by fitting to Eq. (8)) using the following expression:

$$\overline{L}_i' = \overline{L}_i \bullet \frac{f(D_0^*)}{f(D_i^*)} \tag{11}$$

where $\overline{L}_i$ is the mean travel length estimated at node i with Eq. (8), $\overline{L}_i'$ is the mean travel length corrected to account for grain size effects, D_0* is the average ratio (~0.49) between the mean tracer size and median bed size at the site where tracers were seeded (and where Eq. (8) was calibrated), D_i* is the ratio between the median size of augmented and bed sediment at each node and $f(D^*)$ refers to the regression between travel distance and grain size observed by Vázquez-Tarrío et al. (2019a, 2019b):

$$L^* = e^{-0.26 \bullet D^* + 0.26} \tag{12}$$

Once the critical Shields stress for inception of motion was defined and Eq. (8) was calibrated with the available tracer data, we were ready to estimate the mean travel distance of the augmented gravels at each node of the model grid. To do this, we first estimated the critical discharge at each node using Eq. (10), then applied the calibrated Eqs. (8) and (11) to the flow duration curve of the study reach and weighted the outputs by their frequency of recurrence to estimate an average annual distance of travel of the augmented sediment. This estimate is a good approximation of the annually-averaged advective or translating component of the sediment wave propagation. To estimate the dispersive component once the mean travel lengths had been computed, we assigned the travel length distributions around the mean to each node, using either an exponential or gamma distribution. To test the sensitivity of our model to the choice of frequency distribution, we tested both exponential and gamma probability distributions.

When particle travel lengths were normalized by the mean travel distance, the empirical cumulative distribution showed a reasonable visual fit to an exponential distribution with a rate parameter of 1, particularly in case of survey 2 (Fig. 6). The empirical distribution of normalized travel distances also showed a comparable visual fit to a

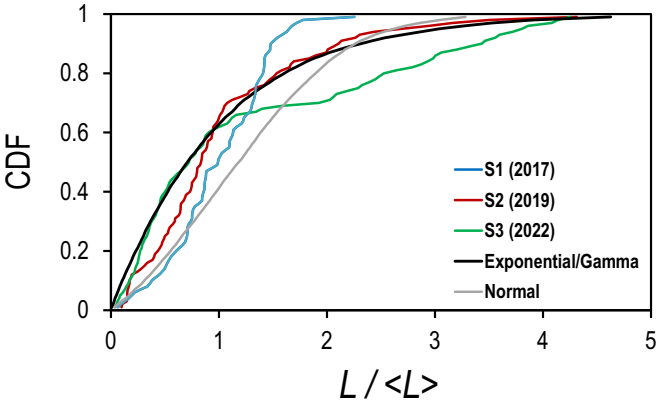

Fig. 6. Comparisons between the empirical cumulative distributions (CDF) of tracer displacements in the different surveys and three theorical probability distributions: exponential, gamma, and normal distributions. Tracer travel lengths were normalized by the mean travel distance ($<L>$). The fitted exponential and gamma distributions overlap in the plot.

gamma distribution (rate and shape parameters equal to 1.1). Indeed, the shapes of the fitted exponential and gamma distributions were almost the same, and both distributions showed a similar adjustment to the empirical data. The exponential and gamma distributions showed better fits to the empirical distribution of travel lengths on the second survey. In the third survey, some departures are observed for travel distances larger than the mean, which we interpret as related to a poor retrieval of tracer frontrunners. Moreover, both distributions showed deviations in the first survey, probably because the empirical distribution of tracer displacements was biased by the loss of tracers caused by signal collision. In addition, we also compared the empirical distribution of tracer displacements with the normal distribution, in view of its widespread use in environmental sciences to represent the values of variables whose distribution is not known a priori. However, visual comparison shows that the normal distribution deviates more from the empirical distributions of the second and third surveys than do the exponential and gamma distributions.

3.5. Stating of sediment-routing rules

Once the bedload transport capacities and the particle travel distances at each node were defined, the last step was to combine both estimates to model the propagation of the injected sediment from the upstream to downstream nodes. To do this, we defined a set of rules to reproduce, in a simple manner, the behavior of bedload during fluvial gravel propagation. During the first model run, we considered a stock of 6885 m^3 of augmented gravel at the most upstream node with all other nodes being empty. Then, the model recruited a volume V of augmented gravel into the bedload, from the first node, according to the following rules:

- If the average annual bedload transport volume (Q_s) at the node is larger than the volume of gravels stocked in the node ($V_{stocked}$), then V is equal to $V_{stocked}$ (all sediment in the node is mobilized);
- If Q_s is lower than $V_{stocked}$, then $V = Q_s$. Consequently, a volume equal to $V_{stocked} - Q_s$ will remain stocked within the node (thereby present for the next model run).

Once recruited by the model, the volume V of entrained gravel is displaced to the downstream nodes according to the travel length distribution associated with the departing node. The outcomes of this first run were used as departing conditions for a second run, in which the former rules were applied to every node stocking augmented gravel. This procedure was repeated successively over 50 runs, each run representing or simulating one hydrological year. In other words, we modelled or simulated the behavior of the augmented gravels over the first 50 yr following the replenishment operation.

At this point, it should be noted that previous tracer research has outlined how sediment propagation slows down with time (Ferguson and Hoey, 2002; Ferguson et al., 2002; Haschenburger, 2013), probably because of the vertical mixing and particle exchange (hereinafter called burial) between the riverbed and the travelling gravels (Haschenburger, 2011, 2012; Houbrechts et al., 2015; Pelosi et al., 2016; Wu et al., 2019; Pierce and Hassan, 2020). To try to incorporate this behavior into our model, at the end of each model run we incorporated or 'buried' a certain volume V_{buried} of augmented gravels into the bed at each node. This volume was computed using:

$$V_{buried} = p_b \bullet V_{arrived} \tag{13}$$

where $V_{arrived}$ is the volume of augmented gravels arriving at a given node from the upstream nodes during a given run of the model. The parameter p_b represents the probability of a given particle of augmented gravel becoming buried or mixed in the bed over the course of one year. This parameter is difficult to quantify because of the complexities inherent to modelling or quantifying active layer fluctuations (Church and Haschenburger, 2017; Ashmore et al., 2018; Vázquez-Tarrío et al., 2021). Therefore, we decided to estimate this parameter according to the ratio of tracer loss during field surveys. Indeed, the ratio of lost tracers provides a maximum estimate for this parameter as long as the tracers are lost not only because of vertical mixing and particle exchange with the bed, but also because of signal collision between them, loss of frontrunners, and/or incomplete prospection (MacVicar and Papangelakis, 2022).

Once incorporated into the bed, the buried sediment will be mobilized during successive model runs only when all the non-buried gravels (at a given node) have been evacuated. The annual volumes of unburied and moved sediment were estimated from:

$$V_{unburied} = d \bullet Mob \bullet V_{buried} \tag{14}$$

where $V_{unburied}$ is the annually-averaged volume of (previously buried) augmented gravel that is unburied or scoured from the bed, Mob is the proportion of bed sediment being mobilized (on average) every year, and d is what we call the 'dilution' parameter, which quantifies the fraction of the bed sediment represented by the (buried) augmented gravels. The Mob and d parameters are estimated as follows:

$$Mob = \frac{Q_{s_{bed}}}{V_{bed}} \tag{15}$$

and

$$d = \frac{V_{buried}}{V_{bed}} \tag{16}$$

where Q_{sbed} is the average annual bedload volume estimated for the bed sediment and V_{bed} is the total volume represented by the stratum of bed sediment, estimated as:

$$V_{bed} = Sp \bullet w \bullet 2 \bullet D_{90} \tag{17}$$

where Sp is the spacing between nodes and D_{90} is the 90th percentile of the surface grain size distribution. In this procedure, we implicitly assumed that buried gravels were incorporated into an active layer with a thickness twice the D_{90}, which seems a good approximation for the typical depths observed for the active-bed layer of gravel-bed rivers (Vázquez-Tarrío et al., 2021).

4. Sensitivity analysis

Prior to applying our modelling approach to solve our specific study question (*what is the time taken by the augmented sediment to reach the downstream reservoir?*), it was sensible to perform a sensitivity analysis. Our aim was to understand how model outcomes may eventually be affected by our choices for the different model parameters, such as the grid spacing, and the travel distance model. This analysis should help us to better interpret the model results. Therefore, we pre-identified five main parameters that could influence the results of our model: (1) the spacing between the nodes in the modelling grid; (2) the regression model used to estimate the mean annual travel distances; (3) the probability distribution used to approximate the distribution of particle travel distances; (4) the value assumed for the probability of tracer burial; and (5) the volumes of augmented sediment injected into the upstream node. Then, prior to interpreting the model outcomes, we evaluated the influence of each of these five factors.

4.1. The spacing between nodes

We ran the model using seven different lengths for the spacing between nodes in the modelling grid: 10, 25, 50, 100, 250, 500, and 1000 m. Two different metrics were used for the comparison. First, the streamwise displacement of the sediment plume centroid ($\overline{L}_c$) was estimated as:

$$\overline{L}_c = \sum_{i=0}^{i=f} L_i \bullet \frac{V_{stocked_i}}{V_{tot}} \quad (18)$$

where L_i is the streamwise distance of node i relative to the departing node ($i = 0$), f refers to the most downstream node, $V_{stockedi}$ is the volume of sediment stocked at each node at the end of the model run, and V_{tot} is the total volume of augmented sediment. The second metric (SD) is the spread or standard deviation of the sediment displacement:

$$SD = \sum_{i=0}^{i=f} |L_i - \overline{L}_c| \bullet \frac{V_{stocked_i}}{V_{tot}} \quad (19)$$

The propagation of sediment waves or plumes along river channels is normally described as a combination of advection (translation) and dispersion (spread) (Lisle et al., 1997; Sklar et al., 2009; Gaeuman et al., 2017). Therefore, the first metric ($\overline{L}_c$) quantifies the advective component of the sediment plume displacements, while the second metric (SD) constitutes a proxy for the sediment plume dispersion (spread).

Comparisons between the outcomes obtained with the different grids show no differences in either the sediment centroid displacement or the SD of sediment displacements for grid spacings below 50 m (Table 3, Fig. 7), i.e., the results obtained with 10-m, 25-m, and 50-m grid spacings were more or less equivalent. For grid spacings above 100 m, the comparison of results clearly shows a decrease in the magnitude of $\overline{L}_c$ with an increase in the spacing between nodes (Fig. 7A). Similarly, we also observed differences in the magnitude of sediment dispersion in the outcomes obtained with the different grids, with an overall increase in the SD in association with an increase in the spacing between nodes up to grid spacings around 100 m; above this value, SD starts to decrease (Fig. 7B).

Hence, as initially expected, when the spacing between nodes is larger than the average displacement of the augmented sediment, the model stocks sediment in the nodes and slows down the downstream propagation. Consequently, the finer the spacing between nodes is, the less affected are the results by this kind of model artifact. However, fine grid spacings are costlier in terms of computation time. Therefore, according to this analysis, a 50-m grid spacing seemed to be an optimum grid spacing for the present work, as long as finer grids do not give substantially different results.

4.2. Mean travel distances

Tracer data available for the Rhône River show statistically significant power and linear regression fits between mean travel lengths and cumulated excess energy (Fig. 4), so the data are therefore compatible with both regression models. Thus, we decided to test the two regression (linear and power) models to analyze how the choice of a specific regression model may influence the model outcomes. To add another element to the comparison, we also tested a regression equation presented in a previous meta-analysis of published tracer data for gravel-bed rivers (Vázquez-Tarrío et al., 2019b). In this meta-analysis, tracer data for 217 transport episodes in 30 gravel-bed rivers were compiled and analyzed, and demonstrated moderate to strong correlations between travel length and dimensionless peak stream power. Therefore, we applied this regression equation to the different bins of discharge of the flow duration curve available for the study site. The results were weighted by flow recurrence and summed to estimate the mean annual travel length.

The use of a power regression model gives larger values for $\overline{L}_c$ and SD than are obtained with a linear model, which in turn gives larger values than an empirical fit obtained from previous data, such as that reported by Vázquez-Tarrío et al. (2019a, 2019b) (Fig. 8). Lacking more data, it is difficult to conclude which model is the best for estimating the mean travel lengths for our study site. Nevertheless, we decided to use the linear regression model in the present work for three reasons: (1) a linear regression model is perfectly compatible with the available tracer data for the study reach; (2) several previous studies observed statistically robust linear correlations between mean travel distance and cumulated excess energy (Haschenburger, 2013; Papangelakis and Hassan, 2016; Papangelakis et al., 2022); and (3) the linear regression model gives results closer to the empirical fit reported by Vázquez-Tarrío et al. (2019a, 2019b) based on previously published tracer data.

4.3. Distribution of particle travel distances

To evaluate the sensitivity of model outcomes to the choice of a specific probability distribution for tracer displacements, we tested three different probability distributions: exponential, gamma, and normal distributions. The estimated $\overline{L}_c$ and SD were very similar with all three distributions (Fig. 9). Larger differences were observed with the normal distribution, which gives larger translation and dispersion distances for the sediment plume. In summary, the results obtained with exponential and gamma distributions were indistinguishable, while the outcomes obtained with a normal distribution involved faster translation and dispersion of the sediment plume. Because of the wide use of the gamma distribution to describe particle displacements in previous tracer studies, we decided to base our calculations for the present research on this distribution.

4.4. Probability of sediment burial

We also analyzed how model outcomes are influenced by the value of the p_b parameter that quantifies the probability of sediment burial. An increase in the probability of tracer burial involves a decrease in the magnitude of the advective component of sediment displacements (Fig. 10A), but an increase in the magnitude of the dispersive component (Fig. 10B). Sediment burial slows down the downstream propagation of the augmented sediment but gives rise to a larger spread of the sediment plume. Larger differences were observed between values of 0 (no burial) and 0.25 (25 % of sediment is annually buried) for the probability of sediment burial. However, above burial probabilities of 0.25, the increase in the magnitude of p_b seemed to have little impact on the model outcomes.

Table 3
Summary of model estimates obtained using different sizes for the model grid. For this sensitivity analysis, we used a power fit between the mean travel distance and flow energy, a gamma distribution for the distribution of sediment displacements, and a value of 0.5 for the probability of sediment burial. Lc: Mean displacement of the sediment plume centroid. SD: Dispersion of the sediment plume.

Grid size (m)	5 years		10 years		25 years		50 years	
	Lc (m)	SD (m)	Lc (m)	SD (m)	Lc (m)	SD (m)	Lc (m)	SD (m)
10	1706.6	1478.3	3741.7	2402.5	6795.01	3014.3	11,009.5	4112.5
25	1697.1	1477.1	3732.9	2401.7	6786.3	3012.4	10,996.9	4108.5
50	1657.8	1482.9	3641.8	2436.1	6679.5	3082.2	10,885.8	4189.1
100	1561.1	1494.01	3362.2	2535.6	6167.1	3356.8	9867.0	4530.8
250	1442.8	1512.9	3008.8	2617.7	5185.9	3619.2	7663.3	4717.4
500	1416.5	1586.9	2811.8	2646.4	4425.3	3600.9	5672.2	4178.9
1000	1414.4	1648.6	2581.2	2524.5	3765.7	3290.6	4463.0	3630.8

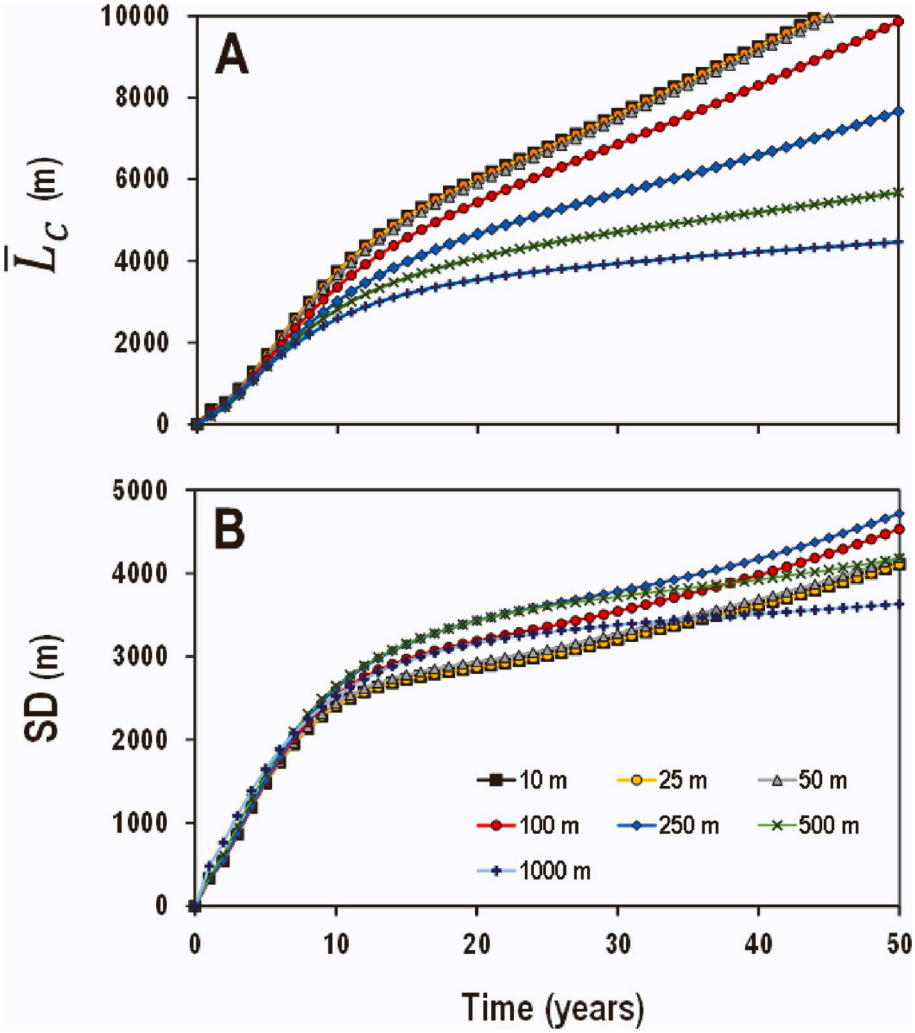

Fig. 7. (A. Upper) Model estimates of the displacement of the sediment plume centroid using different model grids. (B. Lower) Model estimates of the spread (dispersion) of the sediment plume using different model grids. For these simulations, we used a power fit (Fig. 5) between the mean travel distance and flow energy, a gamma distribution for the distribution of sediment displacements, and a value of 0.5 for the probability of sediment burial.

4.5. Sediment volumes injected into the upstream node

As a last step to the sensitivity analysis, we evaluated how the volumes of sediment injected into the upstream node of the grid affected model outcomes and the metrics for sediment displacement. To accomplish this, we performed simulations for four different volumes of sediment introduced into the upstream node: 3000, 6000, 12,000 and 60,000 m^3. These simulations showed a slight increase in $\overline{L}_c$ and SD when the volumes of injected sediment increased from 3000 to 12,000 m^3 (Table 4, Fig. 11). Nevertheless, when the volumes of injected sediment were much larger (60,000 m^3), both $\overline{L}_c$ and SD decreased notably. These results suggest that for volumes of injected sediment much larger than the average bedload capacities at the reach, the stocks in the "rear rank" of the sediment wave contribute to a decrease in the mean displacement of the sediment plume's centroid over a long period of time (Fig. 12).

4.6. Summary results of the sensitivity analysis: defining model parameters

The results of the sensitivity analysis influence the choices for the different steps of the modelling workflow (Fig. 2). Based on this analysis, a 50-m node spacing was considered an optimum choice for the model grid. For the estimation of particle travel distances, we used linear regression between distances and the cumulated excess energy to estimate the mean travel lengths (Fig. 4), combining this with a two-parameter gamma distribution to retrieve the entire distribution of the particle displacements (Fig. 6). For the annual probability of sediment burial, we choose a value of 0.65 based on the average tracer loss in the tracer surveys. However, we should consider that this value provides a maximum estimate for tracer burial as long as tracer loss also involves the loss of frontrunners, signal collision, and an imperfect survey. Nevertheless, above a value of 0.25 for the probability of burial, this parameter seems to have little influence on the model results (Fig. 10).

5. Model results

The model was run using the parameters stated in Section 4.6, and the outcomes provided some interesting results that helped us to understand how the plume of augmented sediment would propagate along the study reach through time. Over the first 10–20 yr, the model predicted a linear increase in the downstream position of the plume centroid (Fig. 13). From approximately 20 yr after the injection of sediment, the advective component of the sediment plume started to slow down, which is clearly illustrated by a change in slope in Fig. 13A. In addition, from 10 yr onwards, the leading front of the sediment wave stops and does not progress farther in the downstream direction, suggesting that the frontrunning sediment had arrived at stable positions

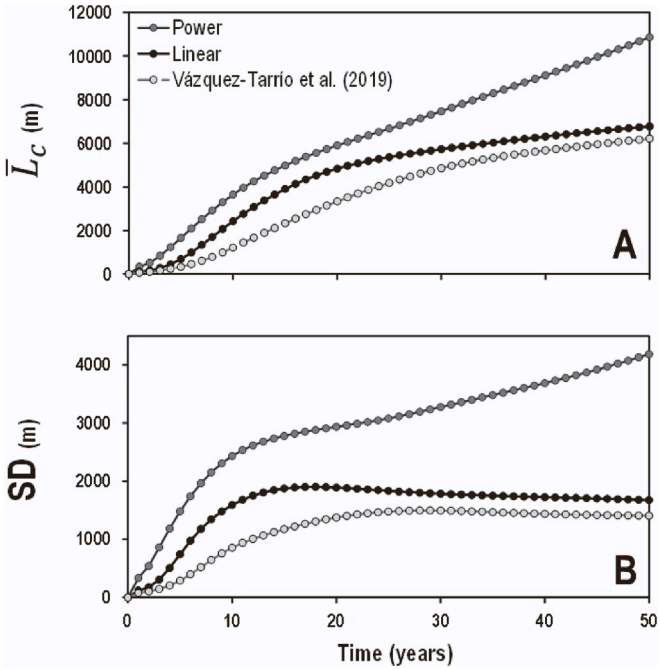

Fig. 8. (A. Upper) Model estimates of the displacement of the sediment plume centroid computed using different models for estimating mean travel lengths at each node of the model grid. (B. Lower) Model estimates of the spread (dispersion) of the sediment plume computed using different models for estimating mean travel lengths at each node of the model grid. For these simulations, we used a 50-m model grid, a gamma distribution for the distribution of sediment displacements, and a value of 0.5 for the probability of sediment burial.

within the channel.

Concerning the dispersive component of the sediment displacements, the model outcomes again showed some interesting results. Over the first 10 yr or so of gravel propagation, the standard deviation of sediment displacements increases linearly with time, i.e., the sediment plume spreads while migrating downstream. Between 10 and 20 yr, the model predicts a change in behavior, with the increase in sediment dispersion starting to slow down. Then, from about 20 yr after the injection of sediment, the change in behavior is more conspicuous and the spread of sediment starts to decrease with time. This suggests that the sediment plume displacement starts to become dominated by translation rather than dispersion. This correlates strongly with the behavior shown by the leading front, which progresses very fast during the first 10 yr of sediment propagation, but slows down severely from 10 yr onwards. This is clearly related to the arrival of the front of the sediment wave at Peyraud weir, where the sudden decrease in slope causes a fall in bedload capacity.

Putting all the above together, it would appear that the model predicts some kind of 'accordion' motion for the progression of the pulse of augmented sediment along the study reach (Fig. 14). With that being said, during the first years after the injection of the gravels, the model predicts that the front of the sediment plume will migrate downstream much faster than the sediment at the tail of the plume. Consequently, the plume of sediment enlarges, i.e., the sediment plume spread increases in parallel with the downstream migration or translation of the sediment wave (Fig. 13A and B). The frontrunning sediment is quickly exported (Fig. 13C), but once the leading front of the sediment reaches the weir, it finds a stable position within the channel. Meanwhile, the downstream progression of sediment continues at the rear of the sediment wave, so that as the sediment that occupies the tail of the sediment plume approaches the leading front, dispersion within the plume of mobile tracers decreases.

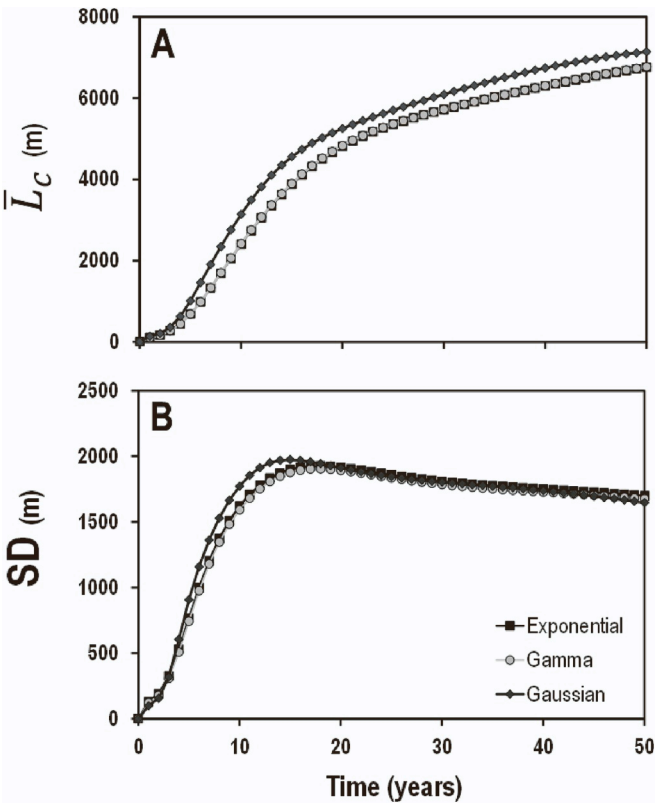

Fig. 9. (A. Upper) Model estimates of the displacement of the sediment plume centroid computed using different probability distributions to predict the entire distribution of sediment travel lengths at each node of the model grid. (B. Lower) Model estimates of the spread (dispersion) of the sediment plume computed using different probability distributions to predict the entire distribution of sediment travel lengths at each node of the model grid. For these simulations, we used a 50-m model grid, a linear fit (Fig. 5) between mean travel distance and flow energy, and a value of 0.5 for the probability of sediment burial.

The model also allows us to analyze how the instream stocks of sediment will evolve in the different compartments of the study reach (Fig. 15). In this regard, the model predicts that even 50 yr after the injection of gravels, the sediment will remain stocked in the upstream bypassed channel, and almost no sediment will arrive at the downstream reservoir. In summary, our simulations show the progressive translation, spread, and fragmentation of the sediment plume through time, and outline how an important amount of sediment will remain stocked in the bypassed channel after 50 yr, and that it will not reach the downstream reservoir. Therefore, it does not seem that a massive arrival of sediment at the downstream reservoir is a real risk or threat, at least in the short term, which was the concern that triggered and motivated the present research.

6. Discussion

6.1. Model expectations and uncertainties

Despite the potential of the workflow proposed in this study to model the downstream propagation of sediment pulses in gravel-bed rivers, there are some limitations to consider. First, our model does not account for the possibility of vertical changes in bed elevation and slope, nor does it account for the surface grain size of the riverbed following gravel augmentation. In this regard, the addition of gravels into the channel may have an impact on bed level or surface texture. Nevertheless, in our study case, the volumes of augmented sediment (~6500 m^3) seem very low compared with the dimensions and volumes of the riverbed.

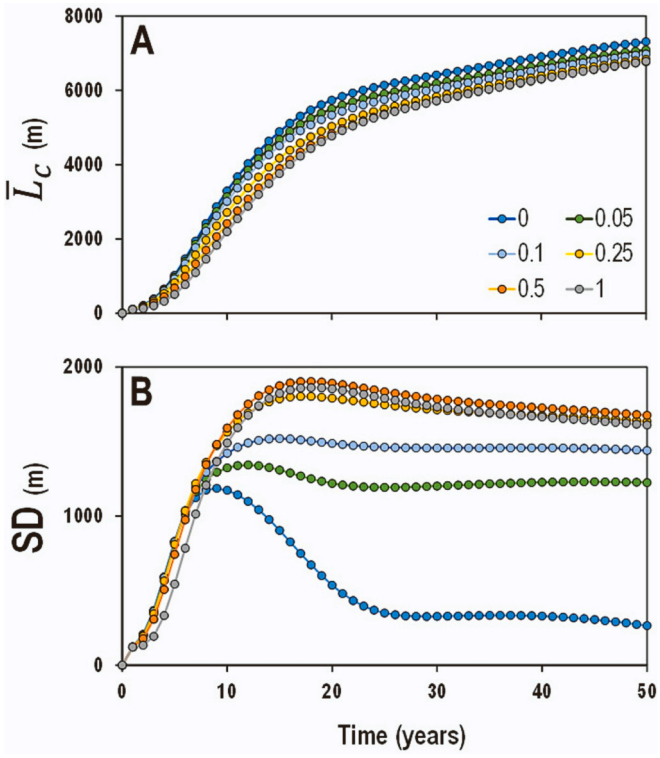

Fig. 10. (A. Upper) Model estimates of the displacement of the sediment plume centroid computed using different probabilities for sediment burial (p_b parameter in Eq. (11)). (B. Lower) Model estimates of the spread (dispersion) of the sediment plume computed using different probabilities of sediment burial. For these simulations, we used a 50-m model grid, a linear fit (Fig. 5) between mean travel distance and flow energy, and a gamma distribution for the distribution of sediment displacements.

Furthermore, the grain size of the injected gravels was finer than that of the bed surface. Thus, we assume that the injected sediment travelled under a regime of sediment supply-limited conditions in the study reach, and both assumptions (no change in bed level or bed size) therefore seem reasonable. However, if larger volumes of sediment replenishment are modelled, or the augmented gravels are coarser than those of the riverbed, we suppose that the sediment wave will propagate under a regime of capacity- or competence-limited conditions, such as in the case shown by the simulation ran with 60,000 m^3 (Fig. 10). In such a case, bed elevation and texture may evolve through time, and the model predictions may therefore deviate from the actual behavior of the channel. Additionally, in all our model runs, we assumed that the depth of particle exchange was constant through time, which we believe is a reasonable choice in our study site. However, in case of bedrock rivers in which the addition of gravel may result in the development of an ephemeral alluvium cover (which will propagate downstream while the sediment pulse migrates), or in case of paved rivers where the addition or large volumes of sand may trigger pavement destabilization (An et al., 2019), this assumption could not be totally adequate and this model parameter (i.e., exchange depth) should be time dependent.

On the other hand, the model proposed here is well developed to simulate the advective and dispersive behavior of a sediment plume, which are the dominant modes for pulse propagation in gravel-bed rivers at the long-term. However, for the time scales normally used in gravel-augmentation works, some studies also reported 'pulse fragmentation' (e.g., Gaeuman et al., 2017). This mechanism involves the original sediment plume breaking into multiple smaller pulses and it has been considered a different mode of sediment-wave propagation. Indeed, our 1D approach could potentially model pulse fragmentation caused by downstream changes in transport capacity (i.e., changes in bed slope, channel width, bed sediment size), but it could be limited in its ability to model pulse fragmentation resulting from the interactions between the travelling sediment and the macro-bedforms; or deriving from changes (triggered by the augmented sediment) in the distribution of in-channel sediment storages and channel morphologies. This concern could be particularly relevant in case of rivers with a great planform development (e.g., wandering, braided). In such cases, sediment augmentation might force deposition and bar formation where sediment is initially absent because of lack of supply, which in turn may affect the bed morphology, modify the bed shear stress distribution and therefore the bedload transport capacity. Nevertheless, in the case of the Rhône River at Péage-de-Roussillon, this concern is limited because several decades of intense river development have led to a fairly simple channel, with scarce macroforms.

Other potential limitations of our model are related to the use of the probability distribution for particle displacements and the choice of the regression model linking mean travel lengths to flow discharge. In tracer experiments, the distributions of travel lengths have commonly been described using an exponential or gamma distribution. Haschenburger (2013) tested several probability distribution functions on data available for Carnation Creek (Canada), but the analysis failed to show a preferred distribution model. The author suggested that more than one probability function could be needed to describe the distributions of path lengths in gravel-bed rivers, and that a specific flood sequence may impact the magnitude of dispersion. Nevertheless, it was also observed that the generalized Pareto and generalized gamma distributions provided the best descriptions of the distribution of displacements in Carnation Creek. In this regard, our comparison between the gamma distribution and the empirical data available for the Rhône River did not show large discrepancies, and we therefore do not believe that this may have greatly impacted our model outcomes.

At our study site, the regression model relating mean travel distances to flow discharge (Eq. (8), Fig. 4) was calibrated with relatively little data. However, there is a long tradition of fluvial geomorphology studies showing that a quasi-linear regression model gives a good description of the displacement of tracers at the reach scale (Haschenburger, 2013; Papangelakis and Hassan, 2016; Papangelakis et al., 2022). Furthermore, comparison with a regression model obtained from a meta-analysis of a large database of previously published data (Vázquez-Tarrío et al., 2019b) suggests that estimates with the linear model do not deviate much from expectations for other rivers.

Key aspects in the design of gravel augmentation operations are the

Table 4
Summary of model estimates computed using different volumes for the sediment injected in the upstream node. For this sensitivity analysis, we used a power fit between the mean travel distance and flow energy, a gamma distribution for the distribution of sediment displacements, and a value of 0.5 for the probability of sediment burial. Lc: Mean displacement of the sediment plume centroid. SD: Dispersion of the sediment plume.

Volumes (m^3)	5 years		10 years		25 years		50 years	
	Lc (m)	SD (m)	Lc (m)	SD (m)	Lc (m)	SD (m)	Lc (m)	SD (m)
3000	705.8	800.6	2271.1	1709.8	4962.4	2221.8	6434.0	2132.5
6500	682.0	743.4	2417.9	1591.2	5361.1	1835.1	6770.5	1676.1
12,000	582.0	643.5	2391.0	1475.3	5568.0	1537.4	6936.4	1359.0
60,000	394.4	536.0	1243.4	1324.0	5222.4	1271.7	6721.5	847.4

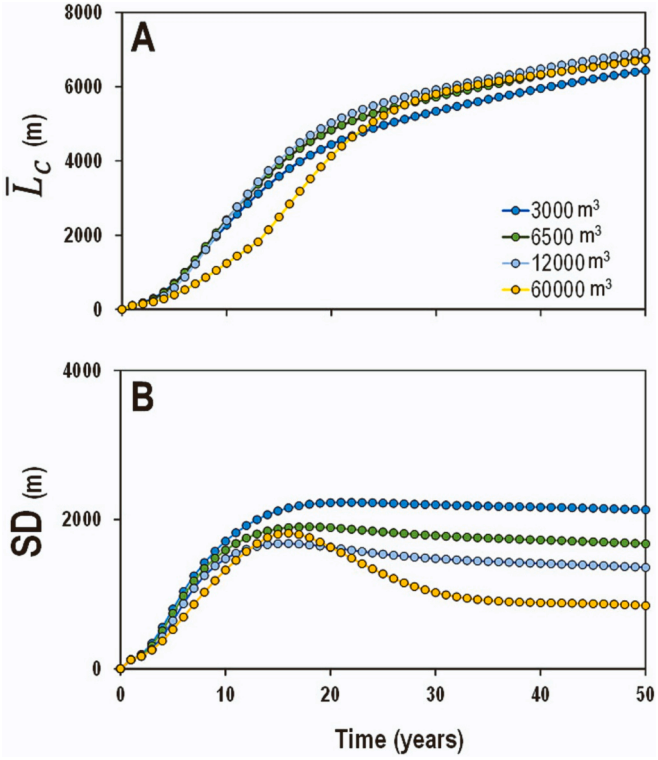

Fig. 11. (A. Upper) Model estimates of the displacement of the sediment plume centroid computed using different volumes for the sediment injected in the upstream node. (B. Lower) Model estimates of the spread (dispersion) of the sediment plume computed using different volumes for the sediment injected in the upstream node. For these simulations, we used a 50-m model grid, a linear fit (Fig. 5) between mean travel distance and flow energy, and a gamma distribution for the distribution of sediment displacements.

optimum location of the replenishment site and the geometry of the stockpile deposit (Chardon et al., 2021). Indeed, previous numerical and physical modelling (Battisacco et al., 2016; Juez et al., 2016) and field studies (Stähly et al., 2019; Chardon et al., 2021) have shown that different geomorphic responses can be obtained, depending on the location and geometry of the stockpile deposit of augmented gravels. According to a study on the Rhine River by Chardon et al. (2021), a prior and detailed 2D assessment of the hydraulic conditions that will erode the stockpile of augmented sediment is needed to optimize the results of gravel augmentation. The 1D approach developed here is unable to address this issue. Nevertheless, a good strategy could be to combine a detailed 2D morphodynamic modelling of the injection site with the workflow proposed in this study. That said, 2D morphodynamical modelling could be used to simulate different scenarios for the geometry of the stockpile deposit at the augmented site, and the results of these simulations could then be used as input parameters at the upstream node of a 1D model, such as the one we propose. In this way, the long-term behavior of different augmentation scenarios could be modelled, helping the decision process when designing augmentation works.

Finally, one major drawback is the lack of data available for validating our model predictions. Validation of the outcomes of our model requires long-term data on sediment displacements and bed level, which are currently unavailable, and it may be some time before they are collected. Nevertheless, a 1D-morphodynamical model implemented in BASEMENT software was calibrated for the study reach by Serlet and Tal (2021), who used it to simulate the long-term behavior of the riverbed in response to gravel augmentation. Their results suggested bed aggradation upstream of the Peyraud weir 50 yr after sediment replenishment, which is congruent with the results obtained with our model. That said, the outcomes of our workflow are also compatible with those of a more "classical" morphodynamic model. In the near future, we expect to apply a similar workflow to other reaches with different characteristics, and to continue performing particle tracking surveys to evaluate the reliability of our proposed modelling strategy in different river settings.

6.2. *Long-term propagation of a sediment wave*

There are not many studies on the long-term tracking and surveying of fluvial gravel displacement. The few available examples include studies on the Alt Dubhaig (Scotland) and on the Carnation Creek (Canada). Ferguson and Hoey (2002) and Ferguson et al. (2002) traced coarse sediment over eight years in the former, whereas Haschenburger (2011, 2013) analyzed particle tracking data for 18 yr of surveys in the latter. Additionally, Houbrechts et al. (2015) tracked the movement of PIT-tagged pebbles on eight medium-sized gravel-bed rivers in Belgium over a period of 5–7 years. These studies reported a progressive advective slow-down of tracers over time, which was probably related to vertical mixing of the sediment within the bed (Haschenburger, 2011,

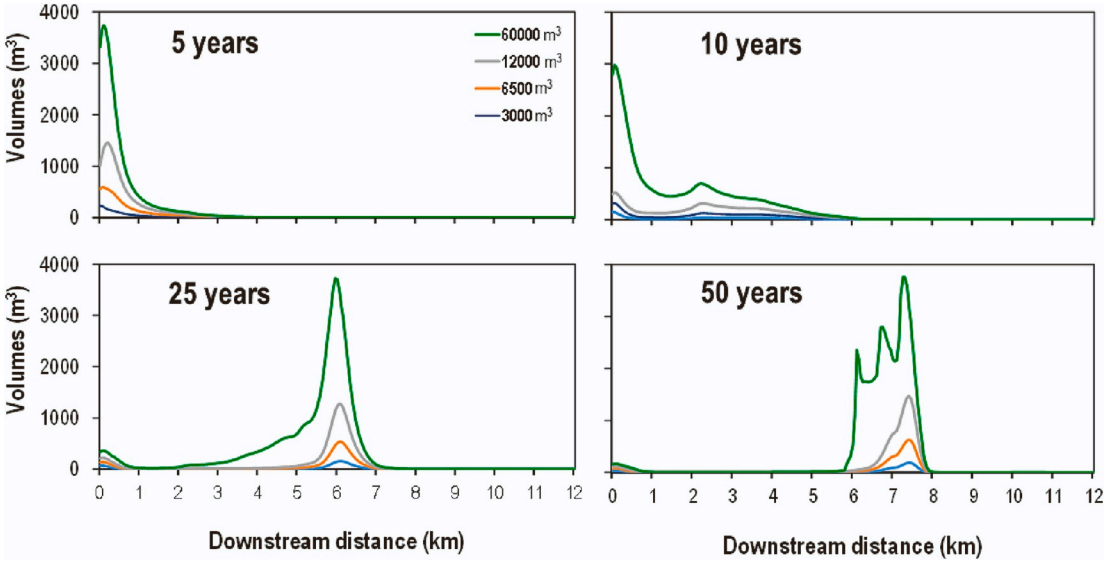

Fig. 12. Model estimates of the volumes of augmented sediment displaced over time along the study reach for different volumes of sediment injected into the upstream node.

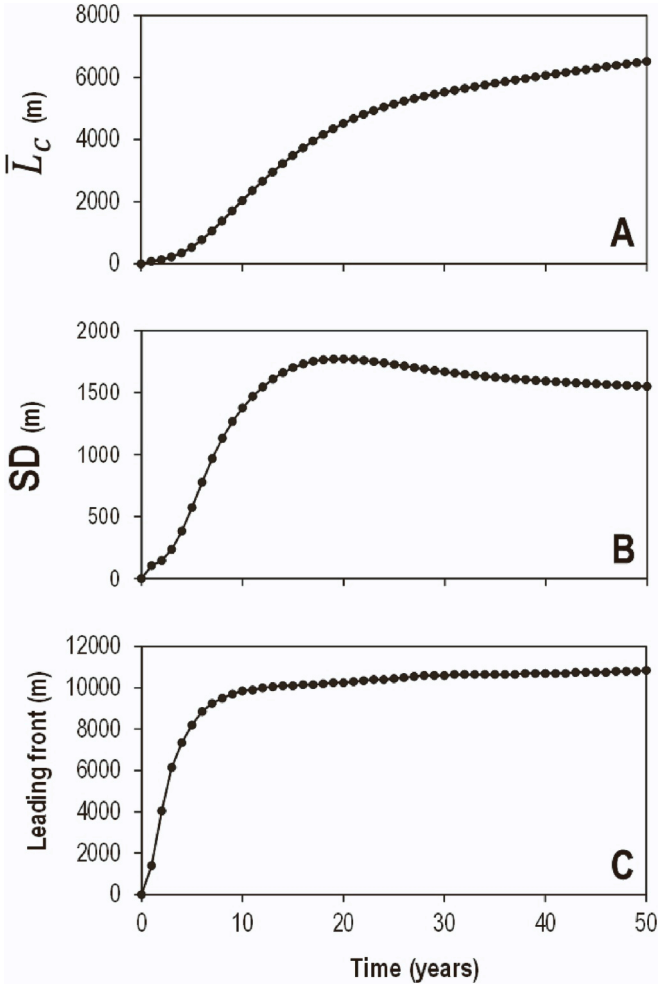

Fig. 13. (A. Upper) Model estimates of the displacement of the sediment plume centroid. (B. Middle) Model estimates of the spread (dispersion) of the sediment plume. (C. Lower). Model estimates of the downstream progression of the leading front of the sediment plume.

2012), as well as with a decrease in the virtual velocity of gravels when they migrate downstream in a concave river profile (Ferguson and Wathen, 1998).

In this sense, given the difficulty of observing the long-term behavior of sediment in the field, a model such as the one proposed here provides a good strategy for its study, and like the results of the studies described above, our model predicts an advective slow down (Fig. 13A). During the first 1–5 yr, the propagation distances increase quickly with time with the incorporation of the unconstrained sediment from the stockpile into the bedload. Once all the sediment is incorporated and mobilized, we predict a rapid drop in sediment propagation velocity such that after 20 yr the velocity is about 20 % of the initial velocity (Fig. 16), which is comparable with the decay in virtual velocities observed by Haschenburger (2011) in Carnation Creek. Thus, comparisons between the outcomes of our model for a scenario with no-vertical mixing and different scenarios of vertical mixing show the potential effects that both sediment burial and a downstream decrease in virtual velocity may have on the propagation of the sediment pulse (Fig. 10A). Our model confirms that vertical mixing has a clear impact on the magnitude of sediment advection (Fig. 10A), and also on the of sediment dispersion (Fig. 10B).

Moreover, the model also provides interesting information on how the shape of the sediment plume evolves over time. As discussed above, from a physical point of view, the movement of a sediment pulse in a gravel-bed river can be understood as an advection/dispersion process. In the first years following gravel augmentation, our model predicts a combination of both spread (dispersion) and translation (advection). There then comes a moment when the leading front arrives at stable positions in the river profile, while the tail and rearguard of the sediment plume continue to migrate downstream. The net result is that the spread of the sediment pulse starts to decrease with time (Fig. 13), while the net translation of the sediment wave decreases severely. Our results clearly show how a downstream change in hydraulic conditions affects and controls sediment wave propagation. That said, the downstream conveyance of the leading front of the augmentation plume is dramatically stopped on arrival at the Peyraud weir, facilitating the regrouping of the sediment at the rearguard with the main plume, and reducing both its translational velocity and dispersion component. To better understand how Peyraud weir affects the pulse propagation while the gravel approaches the weir, we repeated the model excluding the effect of the weir on the hydraulics (Fig. 17). Result of this simulation clearly shows and confirm how both the mean travel distance and the spread of the tracer plume would be larger if the weir were not present.

Temporal changes in the variance of particle travel lengths have been used to characterize the dispersion modes of sediment plumes. Thus, according to Phillips et al. (2013), Hassan et al. (2013), and Hassan and Bradley (2017), the modality of particle transport can be defined according to the correlation between the variance of particle positions (σ^2) and travel time (t):

$$\sigma^2 \sim t^{\gamma} \tag{20}$$

where three different situations can be identified: (1) normal diffusion ($\gamma = 1$), where the sediment plume evolves according to a linear combination of translation and spread; (2) superdiffusion ($\gamma > 1$), where sediment dispersion dominates over translation so that the sediment plume tends to spread or enlarge over time; and (3) subdiffusion ($\gamma < 1$), where the sediment spread is slow and the migration of the sediment plume is dominated by translation. In this sense, the model results show a transition in the behavior of the sediment plume from a superdiffusive to a subdiffusive regime (Fig. 18). The model also allows us to explore the influence that the interactions of the sediment with the bed have on the diffusive regime of the sediment plume. For example, comparisons between the model results when there is no burial and the results obtained with different burial scenarios show a much sharper transition to subdiffusive behavior and a greater predominance of advection when sediment does not interact with the bed (Fig. 13). Nevertheless, the transition from superdiffusion to subdiffusion is present in all the different scenarios of tracer burial, and this change in behavior may therefore be mainly driven by the downstream change in slope and sediment velocities.

In this regard, superdiffusive behavior of sediment plumes in gravel-bed rivers has been explained by wide or heavy-tailed distributions of travel distances (Hassan et al., 2013; Hassan and Bradley, 2017). In simple terms, this means that particles starting from advantageous positions tend to remain in advantageous positions during transport, whereas particles starting from 'handicap' positions tend to remain in 'slow paths'. As a result, at each stage of transport, the faster particles move farther and farther away from the slower particles. This is illustrated in our results for the behavior of the leading front (Fig. 13B). During the first 10 yr, it progresses very fast downstream and a superdiffusive behavior emerges until stable positions are reached and it is dramatically slowed down. From this moment, the sediment plume starts to show a transition to subdiffusive behavior. Nevertheless, sediment burial and vertical mixing involves a smoother transition from superdiffusion to subdiffusion, suggesting that burial decreases the rate at which the tail of the sediment plume migrates in the streamwise direction.

In summary, the scientific literature contains much discussion on how sediment translates and spreads over time in a gravel-bed river. Our model provides results that are congruent and consistent with previous work, but at the same time allows modelling of the long-term behavior

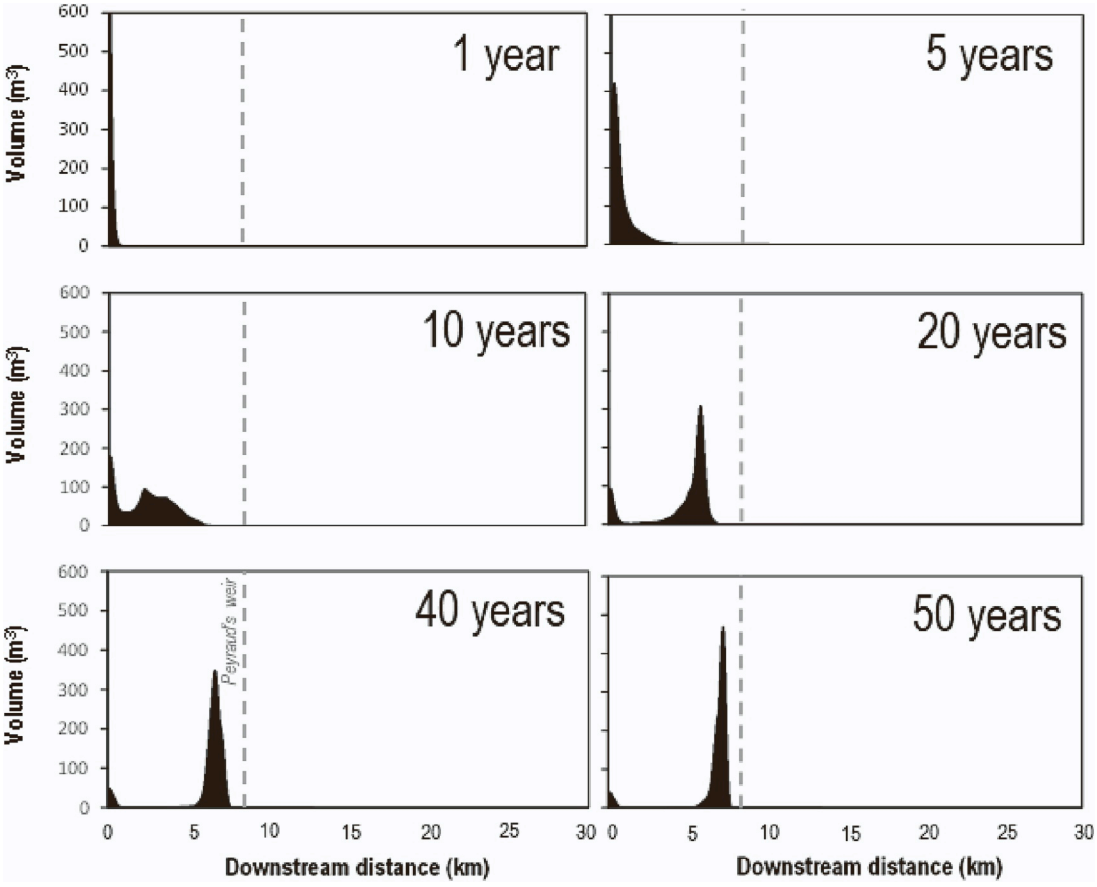

Fig. 14. Model estimates of the volumes of augmented sediment displaced over time along the study reach. The upstream and downstream boundaries of the x-axis are the St. Pierre-de-Boeuf and Arras dams, respectively.

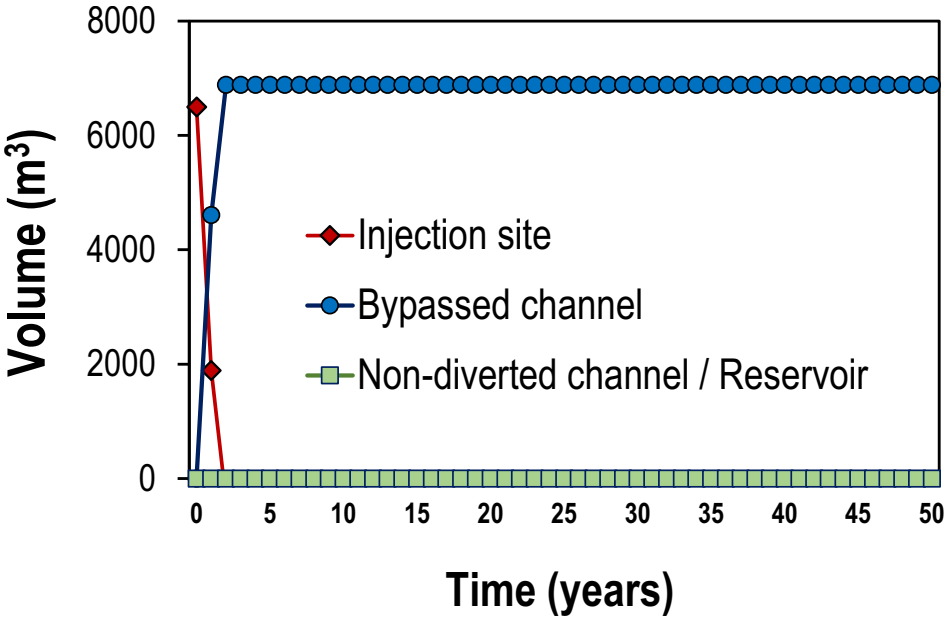

Fig. 15. Summary of model estimates of the volumes of augmented sediment stocked in the different sectors of the study reach.

of a sediment plume, something that is not easy to address with field-work. In this sense, our results show that the degree of interactions of the sediment with the bed and the downstream changes in transport capacity have a significant influence on the modalities of propagation of a pulse of augmented sediment.

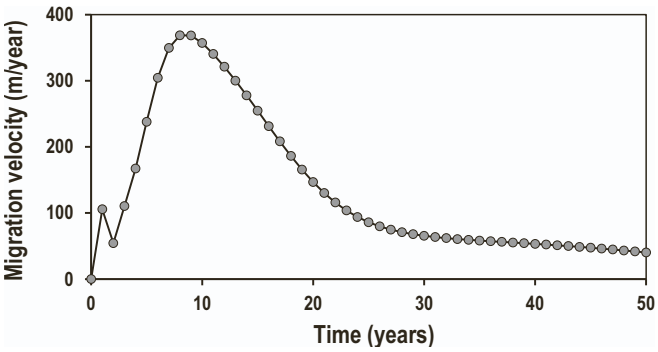

Fig. 16. Model estimates of the velocity of migration of the sediment plume centroid along the study reach.

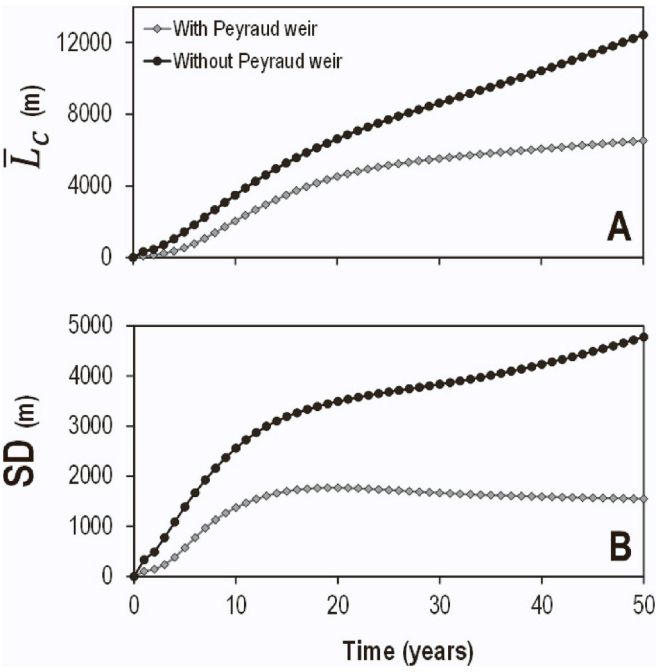

Fig. 17. Comparison between the model estimates obtained considering and not considering the hydraulic effects of Peyraud weir. (A. Upper) Model estimates of the displacement of the sediment plume centroid. (B. Lower) Model estimates of the spread (dispersion) of the sediment plume.

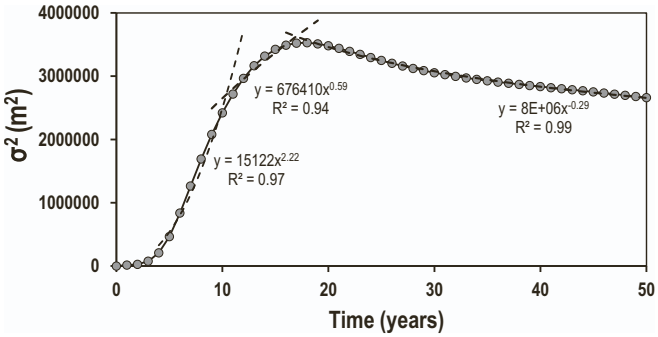

Fig. 18. Model estimates of the variance of sediment displacements.

6.3. Potential practical applications

As indicated earlier, dams and gravel mining often result in the reduction and withdrawal of sediment from the channel and the disruption of the longitudinal continuity of sediment fluxes. Within this context, gravel augmentation is becoming an increasingly common restoration practice for mitigating the sediment starvation associated with these pressures (Arnaud et al., 2017; Brousse et al., 2020). Such a restoration option is therefore effective for restoring and recovering the diversity of fluvial bedforms and the bed state, i.e., for improving river ecological functioning (Wheaton et al., 2004; Ock et al., 2013; Chardon et al., 2021), and is now becoming commonly applied for improving physical habitat (Arnaud et al., 2017; Chardon et al., 2021).

However, gravel replenishment still remains an experimental measure associated with large uncertainties (Harvey et al., 2005; Gaeuman, 2012; Arnaud et al., 2017). In the early stages of gravel replenishment projects, river engineers in charge of gravel augmentation are commonly faced with questions about the optimum volumes, particle sizes, and locations for the replenishment sediment, as well as many other issues. In this regard, we still lack a systematic framework to address many of these questions before acting (Arnaud et al., 2017), and for assessing the pros and cons of different augmentation scenarios. In the case of highly managed rivers, one single and punctual replenishment operation is likely to be insufficient to achieve the expected geomorphic improvements in terms of the diversity of bedforms, grain size, and hydraulic conditions. Successive injections of sediment are probably needed, which raises questions about the right volumes and the optimum injection frequency required to reach the restoration goals when designing gravel augmentation works (Arnaud et al., 2017).

The answers to some of these questions necessarily involve quantification of the travel distance of the sediment, which as we have seen, is an elusive problem in river science. We believe that the framework developed here is very promising and has great potential for providing these elements of scientific knowledge, which can then be fed into the discussion on these issues, helping in the near-future design of gravel augmentation operations in the Rhône River, and potentially in other rivers. Our workflow makes it possible to track the displacement of the sediment introduced during gravel augmentation works, which is a major advantage compared to previous morphodynamical models that are best suited to track changes through time in the topography of the riverbed (aggradational/degradational), as a function of the spatial gradient in sediment transport rates. Availability of models able to simulate the distances of propagation of the sediment incorporated during gravel-augmentation operations, such as the model proposed here, is capital for estimating the adequate volumes and dimensions of the sediment stockpile, and for a better design of sediment replenishment activities, which are key questions within the particular context of the Rhône River and many other rivers worldwide.

7. Conclusions

A century and a half of intense human management has led to a general state of sediment starvation and hydraulic fragmentation in the Rhône River. In an attempt to mitigate this situation, gravel augmentation operations have been carried out in different sectors of the river. One such augmentation was performed in the reach at Péage-de-Roussillon (France), which formed the study site for the present research. Gravel augmentation in this sector raised important concerns from river managers because of the potential threats associated with the hypothesized arrival of large volumes of augmented sediment at a downstream reservoir. Thus, river managers requested information on the time duration over which the augmented sediment would arrive at a downstream reservoir.

Within this context, we developed a modelling framework that makes it possible to simulate the behavior of a pulse of augmented gravel within the study reach. Our method is based on combining bedload transport estimates with estimates of the probability distributions of propagation distances, inferred from particle tracking data collected in the field. With this workflow, we characterized the behavior of the sediment plume over the following 50 yr. The model outcomes are

consistent with previous research on how sediment propagates in gravel-bed rivers.

We believe that our approach shows much promise for the modelling of different scenarios of gravel augmentation, as well as for exploring the long-term displacement and dispersion of sediment in gravel-bed rivers. In this regard, we believe that the methodology developed in this study can be extrapolated to other study cases in other rivers.

Declaration of competing interest

The authors declare that they have no known competing financial interests or personal relationships that could have appeared to influence the work reported in this paper.

Data availability

Data will be made available on request.

Acknowledgments

This study was conducted as part of the Rhône Sediment Observatory (OSR) program, a multi-partner research program funded through the Plan Rhône of the European Regional Development Fund (ERDF), Agence de l'eau Rhône Méditerranée Corse, CNR, EDF, and three regional councils (Region Auvergne-Rhône-Alpes, PACA, and Occitanie). The work was performed within the framework of the EUR H2O'Lyon (ANR-17-EURE-0018) of Université de Lyon (UdL) through the "Investissements d'Avenir" program operated by the French National Research Agency (ANR) and through the Labex DRIIHM French program "Investissements d'Avenir" (ANR-11-LABX-0010) of the Observatoire Hommes-Milieux Vallée du Rhône (OHM VR) managed by the ANR. The first author was also supported by the Spanish Ministry of Science and Innovation (Grants PID2020-116896RB-C21 and PID2020-116896RB-C22 funded by MCIN/AEI/10.13039/501100011033) and the grant PID2021-125938OA-100. Part of this research also benefited from the methods and outcomes of the MorphHab (PID2019-104979RB-I00/AEI/10.13039/501100011033) and PARANTAR (PID2020-115269GB-I00) (MICINN, Gobierno de España) research projects. First author would also like to thank Armando García-Mendoza and Francisco del Salto for their unforgettable science teachings and fruitful exchanges. Finally, we would like to thank associate editor Scott Lecce and the two anonymous reviewers by their comments and suggestions that helped improving the manuscript.

References

Ahammad, M., Czuba, J.A., Pfeiffer, A.M., Murphy, B.P., Belmont, P., 2021. Simulated dynamics of mixed versus uniform grain size sediment pulses in a gravel-bedded river. J.Geophys.Res.Earth Surf. 126 (10), e2021JF006194 https://doi.org/10.1029/2021JF006194.

An, C., Parker, G., Hassan, M.A., Fu, X., 2019. Can magic sand cause massive degradation of a gravel-bed river at the decadal scale? Shi-ting River, China. Geomorphology 327, 147–158.

Arnaud, F., Piégay, H., Béal, D., Collery, P., Vaudor, L., Rollet, A.-J., 2017. Monitoring gravel augmentation in a large regulated river and implications for process-based restoration. Earth Surf. Process. Landf. 42 (13), 2147–2166. https://doi.org/10.1002/esp.4161.

Arnaud, F., Piégay, H., Vaudor, L., Fantino, G., Bultingaire, L., 2015. Technical specifications of low-frequency radio identification bedload tracking from field experiments: differences in antennas, tags and operators. Geomorphology 238, 37–46. https://doi.org/10.1016/j.geomorph.2015.02.029.

Ashmore, P., Peirce, S., Leduc, P., 2018. Expanding the "Active Layer": discussion of Church and Haschenburger (2017) what is the "Active Layer"? Water Resour. Res. 53, 5–10. https://doi.org/10.1002/2016WR019675. Water Resources Research, 54 (3), 1425–1427. doi:10.1002/2017WR022438.

Battisacco, E., Franca, M.J., Schleiss, A.J., 2016. Sediment replenishment: influence of the geometrical configuration on the morphological evolution of channel-bed. Water Resour. Res. 52, 8879–8894. https://doi.org/10.1002/2016WR019157.

Beechie, T.J., 2001. Empirical predictors of annual bed load travel distance, and implications for salmonid habitat restoration and protection. Earth Surf. Process. Landf. 26 (9), 1025–1034. https://doi.org/10.1002/esp.251.

Bradley, D.N., 2017. Direct observation of heavy-tailed storage times of bed load tracer particles causing anomalous superdiffusion. Geophys. Res. Lett. 44 (24), 12227–12235. https://doi.org/10.1002/2017GL075045.

Bradley, N., Tucker, G.E., 2012. Measuring gravel transport and dispersion in a mountain river using passive radio tracers. Earth Surf. Process. Landf. 37, 1034–1045.

Brousse, G., Arnaud-Fassetta, G., Liébault, F., Bertrand, M., Melun, G., Loire, R., et al., 2020. Channel response to sediment replenishment in a large gravel-bed river: the case of the Saint-Sauveur dam in the Buëch River (Southern Alps, France). River Res. Appl. 36 (6), 880–893. https://doi.org/10.1002/rra.3527.

Bunte, K., 2004. State of the science review gravel mitigation and augmentation below hydroelectric dams: a geomorphological perspective. https://doi.org/10.13140/2.1.1094.3361.

Camenen, B., Larson, M., 2005. A general formula for non-cohesive bed load sediment transport. Estuar. Coast. Shelf Sci. 63 (1), 249–260. https://doi.org/10.1016/j.ecss.2004.10.019.

Chardon, V., Schmitt, L., Piégay, H., Arnaud, F., Serouilou, J., Houssier, J., Clutier, A., 2018. Geomorphic effects of gravel augmentation on the Old Rhine River downstream from the Kembs dam (France, Germany). In: E3S Web of Conferences, 40.

Chardon, V., Schmitt, L., Arnaud, F., Piégay, H., Clutier, A., 2021. Efficiency and sustainability of gravel augmentation to restore large regulated rivers: insights from three experiments on the Rhine River (France/Germany). Geomorphology 380, 107639.

Church, M., Haschenburger, J.K., 2017. What is the "active layer"? Water Resour. Res. 53 (1), 5–10. https://doi.org/10.1002/2016WR019675.

Church, M., Hassan, M.A., 1992. Size and distance of travel of unconstrained clasts on a streambed. Water Resour. Res. 28 (1), 299–303. https://doi.org/10.1029/91WR02523.

Cui, Y., 2007. The Unified Gravel-Sand (TUGS) model: simulating sediment transport and gravel/sand grain size distributions in gravel-bedded rivers. Water Resour. Res. 43 (10) https://doi.org/10.1029/2006WR005330.

Cui, Y., Parker, G., Lisle, T.E., Gott, J., Hansler-Ball, M.E., Pizzuto, J.E., et al., 2003. Sediment pulses in mountain rivers: 1. Experiments. Water Resour. Res. 39, 1239. https://doi.org/10.1029/2002WR001803.

Cui, Y., Parker, G., Pizzuto, J., Lisle, T.E., 2003. Sediment pulses in mountain rivers: 2. Comparison between experiments and numerical predictions. Water Resour. Res. 39 (9) https://doi.org/10.1029/2002WR001805.

Cui, Y., Braudrick, C., Dietrich, W.E., Cluer, B., Parker, G., 2006. Dam Removal Express Assessment Models (DREAM). Part 2: Sample runs/sensitivity tests. J. Hydraul. Res. 44 (3), 308–323. https://doi.org/10.1080/00221686.2006.9521684.

Cui, Y., Parker, G., Braudrick, C., Dietrich, W.E., Cluer, B., 2006. Dam Removal Express Assessment Models (DREAM). Part 1: Model development and validation. J. Hydraul. Res. 44 (3), 291–307. https://doi.org/10.1080/00221686.2006.9521683.

Czuba, J.A., 2018. A Lagrangian framework for exploring complexities of mixed-size sediment transport in gravel-bedded river networks. Geomorphology 321, 146–152.

Dade, W.B., Renshaw, C.E., Magilligan, F.J., 2011. Sediment transport constraints on river response to regulation. Geomorphology 126 (1), 245–251. https://doi.org/10.1016/j.geomorph.2010.11.007.

Dépret, T., Piégay, H., Dugué, V., Vaudor, L., Faure, J.-B., Le Coz, J., Camenen, B., 2019. Estimating and restoring bedload transport through a run-of-river reservoir. Sci. Total Environ. 654, 1146–1157. https://doi.org/10.1016/j.scitotenv.2018.11.177.

Dugué, V., Walter, C., Andries, E., Launay, M., Coz, J.L., Camenen, B., Faure, J.B., 2015. In: Accounting for Hydropower Schemes' Operation Rules in the 1D Hydrodynamic Modeling of the Rhône River From Lake Geneva to the Mediterranean Sea, p. 9 https://hal.inrae.fr/hal-02602195.

Ferguson, R.I., Hoey, T.B., 2002. Long-term slowdown of river tracer pebbles: generic models and implications for interpreting short-term tracer studies. Water Resour. Res. 38 (8), 17-1–17-11. https://doi.org/10.1029/2001WR000637.

Ferguson, R.I., Wathen, S.J., 1998. Tracer-pebble movement along a concave river profile: virtual velocity in relation to grain size and shear stress. Water Resour. Res. 34 (8), 2031–2038. https://doi.org/10.1029/98WR01283.

Ferguson, R.I., Bloomer, D.J., Hoey, T.B., Werritty, A., 2002. Mobility of river tracer pebbles over different timescales. Water Resour. Res. 38 (5), 3-1–3-8. https://doi.org/10.1029/2001WR000254.

Gaeuman, D., 2012. Mitigating downstream effects of dams. In: Gravel-bed Rivers. John Wiley & Sons, Ltd., pp. 182–189. https://doi.org/10.1002/9781119952497.ch16

Gaeuman, D., Stewart, R., Schmandt, B., Pryor, C., 2017. Geomorphic response to gravel augmentation and high-flow dam release in the Trinity River,California. Earth Surf. Process. Landf. 42 (15), 2523–2540. https://doi.org/10.1002/esp.4191.

GeoPeka, 2019. Suivi par traçage RFID de la mobilité des sediments d'une operation de reinjection dans le Vieux Rhône de Péage de Roussillon. Rapport final, version 1.3.

Gervasi, A.A., Pasternack, G.B., East, A.E., 2021. Flooding duration and volume more important than peak discharge in explaining 18 years of gravel–cobble river change. Earth Surf. Process. Landf. 46 (15), 3194–3212. https://doi.org/10.1002/esp.5230.

Gibling, M.R., 2018. River systems and the Anthropocene: a late Pleistocene and Holocene timeline for human influence. Quaternary 1 (3), 21. https://doi.org/10.3390/quat1030021.

Gilet, L., Gob, F., Virmoux, C., Gautier, E., Thommeret, N., Jacob-Rousseau, N., 2021. Morpho-sedimentary dynamics associated to dam removal. The Pierre Glissotte dam (central France). Sci. Total Environ. 748, 147079 https://doi.org/10.1016/j.scitotenv.2021.147079.

Grant, G.E., 2012. The geomorphic response of gravel-bed rivers to dams: perspectives and prospects. In: Gravel-bed Rivers. John Wiley & Sons, Ltd., pp. 165–181. https://doi.org/10.1002/9781119952497.ch15

Habersack, H., Piégay, H., 2007. 27 River restoration in the Alps and their surroundings: past experience and future challenges. In: Habersack, H., Piégay, H., Rinaldi, M. (Eds.), Developments in Earth Surface Processes, Vol. 11. Elsevier, pp. 703–735. https://doi.org/10.1016/S0928-2025(07)11161-5.

Harvey, B., McBain, S., Reiser, D., Rempel, L., Sklar, L., Lave, R., 2005. Key Uncertainties in Gravel Augmentation: Geomorphological and Biological Research Needs for Effective River Restoration. CALFED Science and Ecosystem Restoration Programs, Sacramento, CA.

Haschenburger, J.K., 1999. A probability model of scour and fill depths in gravel-bed channels. Water Resour. Res. 35 (9), 2857–2869. https://doi.org/10.1029/1999WR900153.

Haschenburger, J.K., 2011. Vertical mixing of gravel over a long flood series. Earth Surf. Process. Landf. 36 (8), 1044–1058. https://doi.org/10.1002/esp.2130.

Haschenburger, J.K., 2012. On gravel exchange in natural channels. In: Gravel-bed Rivers. John Wiley & Sons, Ltd., pp. 56–67. https://doi.org/10.1002/9781119952497.ch5

Haschenburger, J.K., 2013. Tracing river gravels: insights into dispersion from a long-term field experiment. Geomorphology 200, 121–131. https://doi.org/10.1016/j.geomorph.2013.03.033.

Hassan, M.A., Bradley, D.N., 2017. Geomorphic controls on tracer particle dispersion in gravel-bed rivers. In: Gravel-bed Rivers. John Wiley & Sons, Ltd., pp. 159–184. https://doi.org/10.1002/9781118971437.ch6

Hassan, M.A., Roy, A.G., 2016. Coarse particle tracing in fluvial geomorphology. In: Tools in Fluvial Geomorphology. John Wiley & Sons, Ltd., pp. 306–323. https://doi.org/10.1002/9781118648551.ch14

Hassan, M.A., Church, M., Schick, A.P., 1991. Distance of movement of coarse particles in gravel bed streams. Water Resour. Res. 27 (4), 503–511. https://doi.org/10.1029/90WR02762.

Hassan, M.A., Voepel, H., Schumer, R., Parker, G., Fraccarollo, L., 2013. Displacement characteristics of coarse fluvial bed sediment. J. Geophys. Res. Earth Surf. 118 (1), 155–165. https://doi.org/10.1029/2012JF002374.

Hinton, D., Hotchkiss, R.H., Cope, M., 2018. Comparison of calibrated empirical and semi-empirical methods for bedload transport rate prediction in gravel bed streams. J. Hydraul. Eng. 144 (7), 04018038 https://doi.org/10.1061/(ASCE)HY.1943-7900.0001474.

Houbrechts, G., Levecq, Y., Peeters, A., Hallot, E., Van Campenhout, J., Denis, A.C., Petit, F., 2015. Evaluation of long-term bedload virtual velocity in gravel-bed rivers (Ardenne, Belgium). Geomorphology 251, 6–19.

Juez, C., Battisacco, E., Schleiss, A.J., Franca, M.J., 2016. Assessment of the performance of numerical modeling in reproducing a replenishment of sediments in a water-worked channel. Adv. Water Resour. 92, 10–22. https://doi.org/10.1016/j.advwatres.2016.03.010.

Klösch, M., Habersack, H., 2018. Deriving formulas for an unsteady virtual velocity of bedload tracers. Earth Surf. Process. Landf. 43 (7), 1529–1541. https://doi.org/10.1002/esp.4326.

Kondolf, G.M., 1994. Geomorphic and environmental effects of instream gravel mining. Landsc. Urban Plan. 28 (2–3), 225–243. https://doi.org/10.1016/0169-2046(94)90010-8.

Kondolf, G.M., 1997. PROFILE: hungry water: effects of dams and gravel mining on river channels. Environ. Manag. 21 (4), 533–551. https://doi.org/10.1007/s002679900048.

Kondolf, G.M., Gao, Y., Annandale, G.W., Morris, G.L., Jiang, E., Zhang, J., et al., 2014. Sustainable sediment management in reservoirs and regulated rivers: experiences from five continents. Earth's Future 2 (5), 256–280. https://doi.org/10.1002/2013EF000184.

Lamarre, H., Roy, A.G., 2008. The role of morphology on the displacement of particles in a step–pool river system. Geomorphology 99 (1), 270–279. https://doi.org/10.1016/j.geomorph.2007.11.005.

Lauer, J.W., Viparelli, E., Piégay, H., 2016. Morphodynamics and sediment tracers in 1-D (MAST-1D): 1-D sediment transport that includes exchange with an off-channel sediment reservoir. Adv. Water Resour. 93, 135–149. https://doi.org/10.1016/j.advwatres.2016.01.012.

Launay, M., Dugué, V., Le Coz, J., Camenen, B., Faure, J.B., 2017. Hydro-sedimentary modelling of the Rhône River. Retrieved from. https://hal.inrae.fr/hal-02607085/file/pub00056633.pdf.

Le Coz, J., Camenen, B., Faure, J.-B., Launay, M., Troudet, L., Kieffer, L., et al., 2021. Modélisation des flux – Modèle hydro-sédimentaire 1D (Research Report). Retrieved from. INRAE; IFREMER. https://hal.archives-ouvertes.fr/hal-03293557.

Liébault, F., Bellot, H., Chapuis, M., Klotz, S., Deschâtres, M., 2012. Bedload tracing in a high-sediment-load mountain stream. Earth Surf. Process. Landf. 37 (4), 385–399. https://doi.org/10.1002/esp.2245.

Lisle, T.E., Pizzuto, J.E., Ikeda, H., Iseya, F., Kodama, Y., 1997. Evolution of a sediment wave in an experimental channel. Water Resour. Res. 33 (8), 1971–1981. https://doi.org/10.1029/97WR01180.

Lisle, T.E., Cui, Y., Parker, G., Pizzuto, J.E., Dodd, A.M., 2001. The dominance of dispersion in the evolution of bed material waves in gravel-bed rivers. Earth Surf. Process. Landf. 26 (13), 1409–1420. https://doi.org/10.1002/esp.300.

Loire, R., Piégay, H., Malavoi, J.-R., Kondolf, G.M., Bêche, L.A., 2021. From flushing flows to (eco)morphogenic releases: evolving terminology, practice, and integration into river management. Earth Sci. Rev. 213, 103475 https://doi.org/10.1016/j.earscirev.2020.103475.

MacVicar, B.J., Papangelakis, E., 2022. Lost and found: maximizing the information from a series of bedload tracer surveys. Earth Surf. Process. Landf. 47 (2), 399–408. https://doi.org/10.1002/esp.5255.

Major, J.J., East, A.E., O'Connor, J.E., Grant, G.E., Wilcox, A.C., Magirl, C.S., et al., 2017. Geomorphic responses to dam removal in the United States – a two-decade perspective. In: Gravel-bed Rivers. John Wiley & Sons, Ltd., pp. 355–383. https://doi.org/10.1002/9781118971437.ch13

McQueen, R., Ashmore, P., Millard, T., Goeller, N., 2021. Bed particle displacements and morphological development in a wandering gravel-bed river. Water Resour. Res. 57 (2), e2020WR027850 https://doi.org/10.1029/2020WR027850.

Meyer Peter, Müller, R., 1948. Formulas for bedload transport. In: Proceedings, 2nd Meeting International Association of Hydraulic Research, Stockholm.

Milan, D.J., 2013. Virtual velocity of tracers in a gravel-bed river using size-based competence duration. Geomorphology 198, 107–114. https://doi.org/10.1016/j.geomorph.2013.05.018.

Ock, G., Sumi, T., Takemon, Y., 2013. Sediment replenishment to downstream reaches below dams: implementation perspectives. Hydrol. Res. Lett. 7 (3), 54–59. https://doi.org/10.3178/hrl.7.54.

Olinde, L., Johnson, J.P.L., 2015. Using RFID and accelerometer-embedded tracers to measure probabilities of bed load transport, step lengths, and rest times in a mountain stream. Water Resour. Res. 51 (9), 7572–7589. https://doi.org/10.1002/2014WR016120.

Papangelakis, Elli, Hassan, M.A., 2016. The role of channel morphology on the mobility and dispersion of bed sediment in a small gravel-bed stream. Earth Surf. Process. Landf. 41 (15), 2191–2206. https://doi.org/10.1002/esp.3980.

Papangelakis, E., MacVicar, B.J., Montakhab, A.F., Ashmore, P., 2022. Flow strength and bedload sediment travel distance in gravel bed rivers. Water Resour. Res. 58 (7), e2022WR032296 https://doi.org/10.1029/2022WR032296.

Parrot, E., 2015. Analyse spatio-temporelle de la morphologie du chenal du Rhône du Léman à la Méditerranée (These de doctorat). Lyon 3.

Peeters, A., Houbrechts, G., de le Court, B., Hallot, E., Van Campenhout, J., Petit, F., 2021. Suitability and sustainability of spawning gravel placement in degraded river reaches, Belgium. Catena 201, 105217. https://doi.org/10.1016/j.catena.2021.105217.

Peeters, A., Cassel, M., Vázquez-Tarrío, D., Pont, B., Bounous, M., Mouquet-Noppe, C., Piégay, H., 2022. Évaluation de l'efficacité et de la pérennité de deux actions de restauration de la dynamique sédimentaire sur le Vieux-Rhône de Péage-de-Roussillon. Actes du colloque de la Société Hydrotechnique de France: "Aménagements et biodiversité des cours d'eau", 11 pp.

Pelosi, A., Schumer, R., Parker, G., Ferguson, R.I., 2016. The cause of advective slowdown of tracer pebbles in rivers: Implementation of Exner-based Master Equation for coevolving streamwise and vertical dispersion. J.Geophys.Res.Earth Surf. 121 (3), 623–637. https://doi.org/10.1002/2015JF003497.

Phillips, C.B., Jerolmack, D.J., 2014. Dynamics and mechanics of bed-load tracer particles. Earth Surf.Dyn. 2 (2), 513–530. https://doi.org/10.5194/esurf-2-513-2014.

Phillips, Colin B., Martin, R.L., Jerolmack, D.J., 2013. Impulse framework for unsteady flows reveals superdiffusive bed load transport. Geophys. Res. Lett. 40 (7), 1328–1333. https://doi.org/10.1002/grl.50323.

Phillips, C.B., Hill, K.M., Paola, C., Singer, M.B., Jerolmack, D.J., 2018. Effect of flood hydrograph duration, magnitude, and shape on bed load transport dynamics. Geophys. Res. Lett. 45 (16), 8264–8271. https://doi.org/10.1029/2018GL078976.

Piégay, H., Cottet, M., Lamouroux, N., 2020. Innovative approaches in river management and restoration. River Res. Appl. 36 (6), 875–879. https://doi.org/10.1002/rra.3667.

Pierce, J.K., Hassan, M.A., 2020. Back to Einstein: burial-induced three-range diffusion in fluvial sediment transport. Geophys. Res. Lett. 47 (15), e2020GL087440 https://doi.org/10.1029/2020GL087440.

Pyrce, R.S., Ashmore, P.E., 2003. The relation between particle path length distributions and channel morphology in gravel-bed streams: a synthesis. Geomorphology 56 (1), 167–187. https://doi.org/10.1016/S0169-555X(03)00077-1.

Recking, A., 2013. An analysis of nonlinearity effects on bed load transport prediction. J. Geophys.Res.Earth Surf. 118 (3), 1264–1281. https://doi.org/10.1002/jgrf.20090.

Recking, Alain, Piton, G., Vazquez-Tarrio, D., Parker, G., 2016. Quantifying the morphological print of bedload transport. Earth Surf. Process. Landf. 41 (6), 809–822. https://doi.org/10.1002/esp.3869.

Schmidt, J.C., Wilcock, P.R., 2008. Metrics for assessing the downstream effects of dams. Water Resour. Res. 44 (4) https://doi.org/10.1029/2006WR005092.

Schneider, J.M., Turowski, J.M., Rickenmann, D., Hegglin, R., Arrigo, S., Mao, L., Kirchner, J.W., 2014. Scaling relationships between bed load volumes, transport distances, and stream power in steep mountain channels. J.Geophys.Res.Earth Surf. 119 (3), 533–549. https://doi.org/10.1002/2013JF002874.

Schumm, S.A., Lichty, R.W., 1965. Time, space, and causality in geomorphology. Am. J. Sci. 263 (2), 110–119. https://doi.org/10.2475/ajs.263.2.110.

Serlet, A., Tal, M., 2021. Modélisation morphodynamique 1D du secteur Péage de Roussillon. Rappport de recherche. Aix-Marseille Université.

Sklar, L.S., Fadde, J., Venditti, J.G., Nelson, P., Wydzga, M.A., Cui, Y., Dietrich, W.E., 2009. Translation and dispersion of sediment pulses in flume experiments simulating gravel augmentation below dams. Water Resour. Res. 45 (8) https://doi.org/10.1029/2008WR007346.

Stähly, S., Franca, M.j., Robinson, C.T., Schleiss, A.J., 2019. Sediment replenishment combined with an artificial flood improves river habitats downstream of a dam. Sci. Rep. 9 (1), 5176. https://doi.org/10.1038/s41598-019-41575-6.

Sumi, T., Kantoush, S., Esmaeili, T., Ock, G., 2017. Reservoir sediment flushing and replenishment below dams. In: Gravel-bed Rivers. John Wiley & Sons, Ltd., pp. 385–414. https://doi.org/10.1002/9781118971437.ch14

Syvitski, J., Ángel, J.R., Saito, Y., Overeem, I., Vörösmarty, C.J., Wang, H., Olago, D., 2022. Earth's sediment cycle during the Anthropocene. Nat.Rev.EarthEnviron. 1–18 https://doi.org/10.1038/s43017-021-00253-w.

Vázquez-Tarrío, D., Batalla, R.J., 2019. Assessing controls on the displacement of tracers in gravel-bed rivers. Water 11 (8), 1598. https://doi.org/10.3390/w11081598.

Vázquez-Tarrío, D., Menéndez-Duarte, R., 2015. Assessment of bedload equations using data obtained with tracers in two coarse-bed mountain streams (Narcea River basin, NW Spain). Geomorphology 238, 78–93. https://doi.org/10.1016/j.geomorph.2015.02.032.

Vázquez-Tarrío, D., Menéndez-Duarte, R., 2021. The estimation of bedload in poorly-gauged mountain rivers. Catena 204, 105425. https://doi.org/10.1016/j.catena.2021.105425.

Vázquez-Tarrío, D., Tal, M., Camenen, B., Piégay, H., 2019. Effects of continuous embankments and successive run-of-the-river dams on bedload transport capacities along the Rhône River, France. Sci. Total Environ. 658, 1375–1389. https://doi.org/10.1016/j.scitotenv.2018.12.109.

Vázquez-Tarrío, D., Recking, A., Liébault, F., Tal, M., Menéndez-Duarte, R., 2019. Particle transport in gravel-bed rivers: revisiting passive tracer data. Earth Surf. Process. Landf. 44 (1), 112–128. https://doi.org/10.1002/esp.4484.

Vázquez-Tarrío, D., Piqué, G., Vericat, D., Batalla, R.j., 2021. The active layer in gravel-bed rivers: an empirical appraisal. Earth Surf. Process. Landf. 46 (2), 323–343. https://doi.org/10.1002/esp.5027.

Vázquez-Tarrío, D., Tal, M., Parrot, E., Piégay, H., 2022. Can we incorrectly link armouring to damming? A need to promote hypothesis-driven rather than expert-based approaches in fluvial geomorphology. Geomorphology 413, 108364. https://doi.org/10.1016/j.geomorph.2022.108364.

Viparelli, E., Balkus, A., Vázquez-Tarrío, D., Hill, K.M., Tal, M., Fedele, J., 2022. Streamwise and vertical dispersal of tracer stones in an equilibrium bed. Water Resour. Res. 58, e2022WR033137.

Wheaton, J.M., Pasternack, G.B., Merz, J.E., 2004. Spawning habitat rehabilitation—II. Using hypothesis development and testing in design, Mokelumne River, California, U.S.A. Int. J. River Basin Manag. 2 (1), 21–37. https://doi.org/10.1080/15715124.2004.9635219.

Wilcock, P.R., Crowe, J.C., 2003. Surface-based transport model for mixed-size sediment. J. Hydraul. Eng. 129 (2), 120–128. https://doi.org/10.1061/(ASCE)0733-9429(2003)129:2(120).

Wu, Z., Singh, A., Fu, X., Wang, G., 2019. Transient anomalous diffusion and advective slowdown of bedload tracers by particle burial and exhumation. Water Resour. Res. 55 (10), 7964–7982. https://doi.org/10.1029/2019WR025527.